

ERROR ESTIMATES OF THE FINITE VOLUME SCHEME FOR THE NONLINEAR TENSOR ANISOTROPIC DIFFUSION

OLGA DRBLÍKOVÁ ^{*}, ANGELA HANDLOVIČOVÁ [†], AND KAROL MIKULA [‡]

Abstract. The paper deals with an error analysis of the semi-implicit diamond-cell finite volume scheme, introduced in [4], for solving the nonlinear tensor anisotropic diffusion. First we present the finite volume scheme and its basic properties. Then the error estimate analysis is presented, where the piecewise constant approximation given by the finite volume scheme is compared with the weak solution to the problem. We proved that the error of the approximate solution in L^2 -norm is of order h , where h is a spatial resolution step under the natural relation $k \approx h^2$, where k is a time discretization step. The numerical results devoted to image processing applications are also given.

Key words. Parabolic partial differential equation, nonlinear tensor anisotropic diffusion, image processing, diamond-cell finite volume method, error estimates.

AMS subject classifications. 35K55, 65M12, 74S10, 68U10.

1. Introduction. The nonlinear tensor anisotropic diffusion introduced by Weickert, cf. [20], is used in many image processing applications, cf. [6, 12, 16, 17, 4]. Such model is proper in any situation, where a strong smoothing is useful in a preferred direction, but it should be low in the perpendicular direction. This type of diffusion completes interrupted coherent structures and thus improves the edge detection, cf. [20, 4]. It means that the model is useful to provide image pre-processing for algorithms which depend on edge indicators like the image segmentation, cf. Section 6.

The semi-implicit schemes were introduced to image processing in [8, 19] for solving the regularized Perona-Malik equation, cf. [2, 15]. The finite volume methods were used first time in this context in [13] and adaptivity was developed in [10, 9]. The error estimates for the finite volume discretization of the regularized Perona-Malik model was given in [7]. In [4] the nine point finite volume scheme was designed and studied for solving the nonlinear tensor anisotropic diffusion in image processing. In this paper we prove the error estimates for that scheme. We estimate the difference between approximate and exact solution in dependence on spatial and time discretization step. The main ideas used in our error analysis are a bounding of the gradient in tangential direction by using the gradient in normal direction, a time translate estimate for approximate solution and the Lipschitz continuity of the diffusion tensor elements with respect to the smoothed partial derivatives of the solution.

In section 2 we present the studied mathematical model, its basic properties and provide brief description of the anisotropic diffusion tensor construction. Section 3 is devoted to our semi-implicit diamond-cell finite volume scheme and section 4 summarises important properties of the scheme which are used in the sequel. The core of the paper, the error estimate analysis, is presented in section 5. The paper is finished by a discussion on computational results presented in section 6.

^{*}Department of Mathematics, Faculty of Civil Engineering, Slovak University of Technology, Radlinského 11, 81368 Bratislava, Slovakia (olga.drblikova@stuba.sk).

[†]Department of Mathematics, Faculty of Civil Engineering, Slovak University of Technology, Radlinského 11, 81368 Bratislava, Slovakia (angela.handlovicova@stuba.sk).

[‡] Department of Mathematics, Faculty of Civil Engineering, Slovak University of Technology, Radlinského 11, 81368 Bratislava, Slovakia (karol.mikula@stuba.sk).

2. Mathematical model. The nonlinear tensor anisotropic diffusion model has the following form

$$(2.1) \quad \frac{\partial u}{\partial t} - \nabla \cdot (D \nabla u) = 0, \quad \text{in } Q_T \equiv I \times \Omega,$$

$$(2.2) \quad u(x, 0) = u_0(x), \quad \text{in } \Omega,$$

$$(2.3) \quad D \nabla u \cdot \mathbf{n} = 0, \quad \text{on } I \times \partial \Omega,$$

where an unknown function is given by $u(x, t)$ and represents a grey level image intensity, $I = [0, T]$ denotes a time interval, Ω is a 2D rectangular image domain with boundary $\partial \Omega$, $u_0 \in L^2(\Omega)$ is an initial condition (processed image) and \mathbf{n} is the outer normal unit vector to the $\partial \Omega$. The matrix D represents so-called the diffusion tensor depending on the eigenvalues and eigenvectors of the (regularized) structure tensor

$$(2.4) \quad J_\rho(\nabla u_{\tilde{t}}) = G_\rho * (\nabla u_{\tilde{t}} \nabla u_{\tilde{t}}^T),$$

where $u_{\tilde{t}}(x, t) = (G_{\tilde{t}} * u(\cdot, t))(x)$, ($\tilde{t} > 0$) is used. $G_{\tilde{t}}$ and G_ρ are Gaussian kernels. The matrix J_ρ is symmetric and positive semidefinite and its eigenvectors are parallel and orthogonal to $\nabla u_{\tilde{t}}$, respectively. In computer vision the matrix $J_\rho = \begin{pmatrix} a & b \\ b & c \end{pmatrix}$ is known as a structure tensor or interest operator or second moment matrix. Its eigenvalues are given by

$$(2.5) \quad \mu_{1,2} = \frac{1}{2} \left(a + c \pm \sqrt{(a-c)^2 + 4b^2} \right), \quad \mu_1 \geq \mu_2.$$

The corresponding orthogonal set of eigenvectors (v, w) to eigenvalues (μ_1, μ_2) is given by

$$(2.6) \quad \begin{aligned} v &= (v_1, v_2), & w &= (w_1, w_2), \\ v_1 &= 2b, & v_2 &= c - a + \sqrt{(a-c)^2 + 4b^2}, \\ v \perp w, & & w_1 &= -v_2, & w_2 &= v_1. \end{aligned}$$

The orientation of the eigenvector w , which corresponds to the smaller eigenvalue μ_2 is called coherence orientation. This orientation has the lowest fluctuations in image intensity.

The diffusion tensor D is designed to steer a smoothing process such that the filtering is strong along the coherence direction w and increases with the coherence $(\mu_1 - \mu_2)^2$. To that goal D must possess the same eigenvectors v and w as the structure tensor $J_\rho(\nabla u_{\tilde{t}})$ and the eigenvalues of D are chosen as follows

$$(2.7) \quad \begin{aligned} \kappa_1 &= \alpha, \quad \alpha \in (0, 1), \quad \alpha \ll 1, \\ \kappa_2 &= \begin{cases} \alpha, & \text{if } \mu_1 = \mu_2, \\ \alpha + (1 - \alpha) \exp\left(\frac{-C}{(\mu_1 - \mu_2)^2}\right), & C > 0 \quad \text{else.} \end{cases} \end{aligned}$$

Then D has the following form

$$(2.8) \quad D = ABA^{-1}, \quad \text{where } A = \begin{pmatrix} v_1 & -v_2 \\ v_2 & v_1 \end{pmatrix} \quad \text{and } B = \begin{pmatrix} \kappa_1 & 0 \\ 0 & \kappa_2 \end{pmatrix},$$

so it depends nonlinearly on partial derivatives of solution u , satisfies smoothness, symmetry and uniform positive definiteness properties.

DEFINITION 2.1. A function $u \in L^2(0, T; H^1(\Omega))$ is a weak solution of the problem (2.1)-(2.3) if satisfies the identity

$$(2.9) \quad \int_0^T \int_{\Omega} u \frac{\partial \varphi}{\partial t}(x, t) dx dt + \int_{\Omega} u_0(x) \varphi(x, 0) dx - \int_0^T \int_{\Omega} (D\nabla u) \cdot \nabla \varphi dx dt = 0, \quad \forall \varphi \in \Psi,$$

where

$$(2.10) \quad \Psi = \{ \varphi \in C^{2,1}(\bar{\Omega} \times [0, T]), D\nabla \varphi \cdot \vec{n} = 0 \text{ on } \partial\Omega \times (0, T), \varphi(\cdot, T) = 0 \}.$$

3. The numerical scheme. In order to build the scheme we used the finite volume method, cf. [5], since this discretization technique uses the piecewise constant representation of approximate solutions similarly to the structure of digital images, cf. [13]. The restrictions of the classical five-point methods for the tensor models lead to a choice of the nine-point diamond-cell method, cf. [3, 4].

Let the image be represented by $n_1 \times n_2$ pixels (finite volumes) such that it looks like a mesh with n_1 rows and n_2 columns. Let $\Omega = (0, n_1 h) \times (0, n_2 h)$, h is a pixel size. We consider the smoothing process in a time interval $I = [0, T]$. Let $0 = t_0 \leq t_1 \leq \dots \leq t_{N_{max}} = T$ denote the time discretization with $t_n = t_{n-1} + k$, where k is a length of discrete time step. In our scheme we will look for u^n an approximation of solution at time t_n , for every $n = 1, \dots, N_{max}$. We start with an integration of the equation (2.1) over finite volume W , then provide a semi-implicit time discretization and use a divergence theorem to get

$$(3.1) \quad \frac{u_W^n - u_W^{n-1}}{k} m(W) - \sum_{\sigma \in \mathcal{E}_W \cap \mathcal{E}_{int}} \int_{\sigma} (D^{n-1} \nabla u^n) \cdot \mathbf{n}_{W, \sigma} ds = 0,$$

where u_W^n , $W \in \mathcal{T}_h$, represents the value of u^n on W . \mathcal{T}_h is an admissible finite volume mesh, cf. [5] and further quantities and notations are described as follows: $m(W)$ is the measure of the finite volume W with boundary ∂W , $\sigma_{WE} = W \cap E = W|E$ is an edge of the finite volume W , where $E \in \mathcal{T}_h$ is an adjacent finite volume to W such that $m(W \cap E) \neq 0$. Due to simplifying notation, we use σ instead of σ_{WE} at several places if no confusion can appear (e.g. in (3.1)). \mathcal{E}_W is the set of edges such that $\partial W = \bigcup_{\sigma \in \mathcal{E}_W} \sigma$ and $\mathcal{E} = \bigcup_{W \in \mathcal{T}_h} \mathcal{E}_W$. The set of boundary edges is denoted by \mathcal{E}_{ext} , that is $\mathcal{E}_{ext} = \{ \sigma \in \mathcal{E}, \sigma \subset \partial\Omega \}$ and let $\mathcal{E}_{int} = \mathcal{E} \setminus \mathcal{E}_{ext}$. Υ is the set of pairs of adjacent finite volumes, defined by $\Upsilon = \{ (W, E) \in \mathcal{T}_h^2, W \neq E, m(\sigma_{WE}) \neq 0 \}$ and $\mathbf{n}_{W, \sigma}$ is the normal unit vector to σ outward to W .

Next step is to define our discrete numerical solution by

$$(3.2) \quad u_{h,k}(x, t) = \sum_{n=0}^{N_{max}} \sum_{W \in \mathcal{T}_h} u_W^n \chi\{x \in W\} \chi\{t_{n-1} < t \leq t_n\},$$

where the function $\chi(A)$ is defined as follows

$$(3.3) \quad \chi\{A\} = \begin{cases} 1, & \text{if } A \text{ is true,} \\ 0, & \text{elsewhere.} \end{cases}$$

The extension of the function (3.2) outside Ω is given first by its periodic mirror reflection in $\Omega_{\tilde{t}}$, where \tilde{t} is the width of the smoothing kernel,

$$(3.4) \quad \Omega_{\tilde{t}} = \Omega \cup B_{\tilde{t}}(x), \quad x \in \partial\Omega,$$

$B_{\tilde{t}}(x)$ is a circle centered at x with radius \tilde{t} , and then we extend this periodic mirror reflection by 0 outside $\Omega_{\tilde{t}}$ and denote it by $\tilde{u}_{h,k}$.

We start computations by defining initial values

$$(3.5) \quad u_W^0 = \frac{1}{m(W)} \int_W u_0(x) dx, \quad W \in \mathcal{T}_h$$

and let the finite volume approximation at the n -th time step be given by

$$u_{h,k}^n(x) = \sum_{W \in \mathcal{T}_h} u_W^n \chi\{x \in W\}.$$

In order to get the scheme we write (3.1) in the form

$$\frac{u_W^n - u_W^{n-1}}{k} - \frac{1}{m(W)} \sum_{\sigma \in \mathcal{E}_W \cap \mathcal{E}_{int}} \phi_\sigma^n(u_{h,k}^n) m(\sigma) = 0,$$

where $m(\sigma)$ is the measure of edge σ and $\phi_\sigma^n(u_{h,k}^n)$ denotes an approximation of the exact averaged flux $\frac{1}{m(\sigma)} \int_\sigma (D^{n-1} \nabla u^n) \cdot \mathbf{n}_{W,\sigma} ds$ for any W and $\sigma \in \mathcal{E}_W$.

We construct an approximation of the flux with the help of a co-volume mesh, cf. e.g. [3]. The co-volume χ_σ associated to σ is constructed around each edge by joining endpoints of this edge and midpoints of finite volumes which are common to this edge, see Fig.3.1. Using this method we get the scheme which has the form, cf. [4],

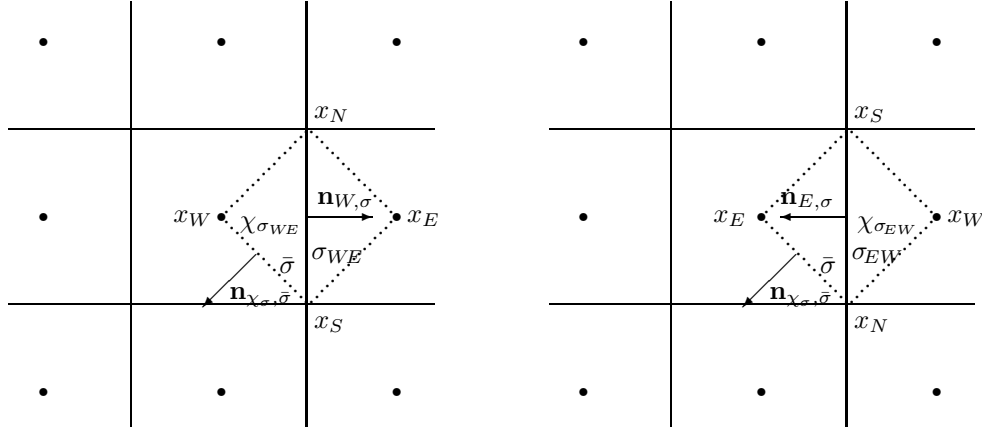


FIG. 3.1. A detail of a mesh. The co-volumes χ_σ associated to edges $\sigma = \sigma_{WE}$ (left) and $\sigma = \sigma_{EW}$ (right).

$$(3.6) \quad \frac{u_W^n - u_W^{n-1}}{k} - \frac{1}{m(W)} \sum_{\sigma \in \mathcal{E}_W \cap \mathcal{E}_{int}} \phi_\sigma^n(u_{h,k}^n) m(\sigma) = 0$$

with

$$(3.7) \quad \phi_\sigma^n(u_{h,k}^n) = \bar{\lambda}_\sigma \frac{u_E^n - u_W^n}{h} + \bar{\beta}_\sigma \frac{u_N^n - u_S^n}{h},$$

where $\bar{\lambda}_\sigma$ and $\bar{\beta}_\sigma$ are elements of the matrix $D_\sigma = D_\sigma^{n-1} = \begin{pmatrix} \bar{\lambda}_\sigma & \bar{\beta}_\sigma \\ \bar{\beta}_\sigma & \bar{\nu}_\sigma \end{pmatrix}$ written in the basis $(\mathbf{n}_{W,\sigma}, \mathbf{t}_{W,\sigma})$, cf. [3], where $\mathbf{t}_{W,\sigma}$ is a unit vector parallel to σ such that $(x_N - x_S) \cdot \mathbf{t}_{W,\sigma} > 0$. Let us note that $\bar{\lambda}_\sigma$ denotes $\bar{\lambda}(u_{h,k})(x_{WE}, t_{n-1})$ and $\bar{\beta}_\sigma$ is given correspondingly, where x_{WE} is a point of $\sigma_{WE} = W|E$ intersecting the segment $x_W x_E$. Even if it may look artificial, it will simplify further considerations. In practice it means that,

$$(3.8) \quad \bar{\lambda}_\sigma = \lambda_\sigma, \quad \bar{\beta}_\sigma = \beta_\sigma \quad \text{and} \quad \bar{\nu}_\sigma = \nu_\sigma \quad \text{for edges parallel to axis } y.$$

On the other hand,

$$(3.9) \quad \bar{\lambda}_\sigma = \nu_\sigma, \quad \bar{\beta}_\sigma = -\beta_\sigma \quad \text{and} \quad \bar{\nu}_\sigma = \lambda_\sigma \quad \text{for edges parallel to axis } x,$$

where $\begin{pmatrix} \lambda_\sigma & \beta_\sigma \\ \beta_\sigma & \nu_\sigma \end{pmatrix}$ are values of the diffusion tensor on edge σ written in the standard basis $((1, 0)^T, (0, 1)^T)$.

The values at x_E and x_W are taken as u_E and u_W , and the values u_S and u_N at the vertices x_N and x_S are computed as the arithmetic mean of u_W , where W are finite volumes which are common to this vertex. Although these u_N^n , u_W^n , u_E^n and u_S^n correspond to particular edge σ , and so we should denote them by $u_{N_\sigma}^n$, $u_{W_\sigma}^n$, $u_{E_\sigma}^n$ and $u_{S_\sigma}^n$ in (3.7), we will use the above simplified notations.

4. Stability and convergence results. The goal of this section is to present results concerning stability and convergence properties for our scheme. All results given in this section were proven in [4], we present them here because they will be also used in section 5 devoted to error estimates for the scheme.

LEMMA 4.1. (Bounding of the gradient in tangential direction) *The gradient in tangential direction can be bounded by the gradient in normal direction (see Fig. 3.1) as follows*

$$(4.1) \quad \sum_{\sigma \in \mathcal{E}_{int}} \left(\frac{\bar{\beta}_\sigma}{\bar{\lambda}_\sigma} \right)^2 \left(\frac{u_N^n - u_S^n}{h} \right)^2 \bar{\lambda}_\sigma \leq \gamma \sum_{\sigma \in \mathcal{E}_{int}} \left(\frac{u_E^n - u_W^n}{h} \right)^2 \bar{\lambda}_\sigma,$$

where $0 \leq \gamma < 1$, $\gamma = \max_{\sigma \in \mathcal{E}} \gamma_\sigma$, $\gamma_\sigma = \sum_{\delta \in P_\sigma \cap \mathcal{E}_{int}} \frac{1}{4} \left(\frac{\bar{\beta}_\delta}{\bar{\lambda}_\delta} \right)^2 \frac{\bar{\lambda}_\delta}{\bar{\lambda}_\sigma}$,

where edges δ and set P_σ are given in the following definition.

DEFINITION 4.2. *Let P_σ be the set of all edges δ perpendicular to σ (see Fig. 4.1 for two illustrative situations when $\sigma = \sigma_{WE}$ and $\sigma = \sigma_{EW}$), which have common vertex with σ and fulfill the following conditions:*

$$(x_{E_\delta} - x_{W_\delta}) \cdot \mathbf{n}_{W,\sigma} > 0 \quad \text{if} \quad (x_{N_\sigma} - x_{S_\sigma}) \cdot \mathbf{t}_{W,\sigma} > 0 \quad \text{and}$$

$$(x_{E_\delta} - x_{W_\delta}) \cdot \mathbf{n}_{W,\sigma} < 0 \quad \text{if} \quad (x_{N_\sigma} - x_{S_\sigma}) \cdot \mathbf{t}_{W,\sigma} < 0.$$

Let us note that $x_{W_\sigma} = x_{W_\delta}^1 = x_{E_\delta}^3$, for $\sigma = \sigma_{WE}$, $x_{E_\sigma} = x_{W_\delta}^2 = x_{E_\delta}^4$, for $\sigma = \sigma_{WE}$, $x_{W_\sigma} = x_{E_\delta}^2 = x_{W_\delta}^4$, for $\sigma = \sigma_{EW}$ and $x_{E_\sigma} = x_{E_\delta}^1 = x_{W_\delta}^3$, for $\sigma = \sigma_{EW}$.

THEOREM 4.3. (Existence and uniqueness of discrete solution) *For h sufficiently small, there exists unique solution $u_{h,k}^n$ given by the scheme (3.6)-(3.7) at any discrete time step t_n .*

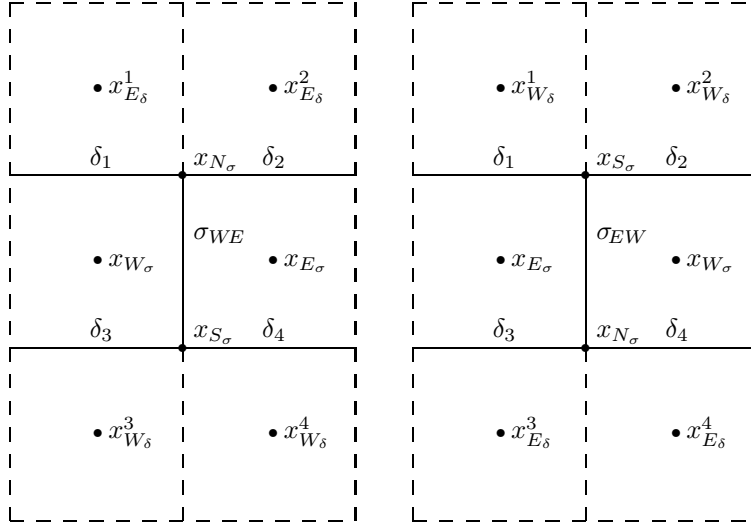


FIG. 4.1. *Left: an edge σ_{WE} and edges $\delta_1, \delta_2, \delta_3, \delta_4 \in P_{\sigma_{WE}}$. Right: an edge σ_{EW} and edges $\delta_1, \delta_2, \delta_3, \delta_4 \in P_{\sigma_{EW}}$.*

The convergence analysis of our scheme was based on Lemma 4.1 and Kolmogorov's compactness criterion in L^2 . The scheme is more complicated in comparison with classical five-point schemes due to "corners points", which are included in the gradient in tangential direction, and we overcame that difficulty with the help of Lemma 4.1. Kolmogorov's compactness theorem, cf. e.g. [5], follows from lemmata 4.4-4.7 and implies relative compactness of the sequence of numerical solutions given by our scheme refining the space and time discretization step. The relative compactness enables us to choose the convergent subsequence which in the limit gives the weak solution.

LEMMA 4.4. **(Uniform boundedness)** *There exists a positive constant C such that*

$$(4.2) \quad \|u_{h,k}\|_{L^2(Q_T)} \leq C.$$

LEMMA 4.5. **(Time translate estimate)** *For any $s \in (0, T)$ there exists a positive constant C such that*

$$(4.3) \quad \int_{\Omega \times (0, T-s)} (u_{h,k}(x, t+s) - u_{h,k}(x, t))^2 dx dt \leq Cs.$$

LEMMA 4.6. **(Space translate estimate I)** *There exists a positive constant C such that*

$$(4.4) \quad \int_{\Omega_\xi \times (0, T)} (u_{h,k}(x + \xi, t) - u_{h,k}(x, t))^2 dx dt \leq C |\xi| (|\xi| + 2h)$$

for any vector $\xi \in R^d$, where $\Omega_\xi = \{x \in \Omega, [x, x + \xi] \in \Omega\}$.

LEMMA 4.7. (**Space translate estimate II**) *There exists a positive constant C such that*

$$(4.5) \quad \int_{\Omega \times (0, T)} (u_{h,k}(x + \xi, t) - u_{h,k}(x, t))^2 dx dt \leq C |\xi|$$

for any vector $\xi \in R^d$.

Finally we state the following theorem from [4].

THEOREM 4.8. (**Convergence of the scheme**) *The sequence $u_{h,k}$ converges strongly in $L^2(Q_T)$ to the unique weak solution u of (2.1)-(2.3) as $h, k \rightarrow 0$.*

5. Error estimates. In this section we are going to derive error estimates between weak solution of the model (2.1)-(2.3) and the numerical solution satisfying the scheme (3.6)-(3.7). For the error analysis a stronger regularity assumptions must be stated than arise in practice, but it is a general approach when deriving the error estimates. By the results presented in [20] we know that weak solution $u \in C^\infty(\bar{\Omega}, (0, \infty))$.

THEOREM 5.1. (**Error estimate**) *Let the weak solution fulfill the following regularity properties: $\nabla u \in L_\infty(Q_T)$, $u_{tt} \in L_2(Q_T)$, $u \in L_2(I, W^{2,2}(\Omega))$, $\nabla u_t \in L_2(I, L_\infty(\Omega))$. Let $e_W^n = u(x_W, t_n) - u_W^n$ and*

$$e_{h,k}^n(x, t) = \sum_{W \in \mathcal{T}_h} e_W^n \chi\{x \in W\} \chi\{t_{n-1} < t \leq t_n\}.$$

Then, there exist a constant C , such that for sufficiently small h

$$(5.1) \quad \int_{\Omega} |e_{h,k}^m|^2 dx + \sum_{n=1}^m \int_{\Omega} |e_{h,k}^n - e_{h,k}^{n-1}|^2 dx + \sum_{n=1}^m \int_{t_{n-1}}^{t_n} \sum_{\sigma \in \mathcal{E}_{int}} (e_E^n - e_W^n)^2 dt \leq C(h^2 + k)$$

for every $m = 1, \dots, N_{\max}$.

Proof. Let us define $\mathcal{P}_0(\mathcal{T}_h)$ as the set of functions from Ω to R which are constant over each finite volume W of the mesh \mathcal{T}_h . Let now $t_{n-1} < t \leq t_n$. We multiply equation (2.1) by $v_W^n \in \mathcal{P}_0(\mathcal{T}_h)$, integrate it over volume W and use divergence theorem to have

$$(5.2) \quad \int_W \partial_t u(x, t) v_W^n dx - \sum_{\sigma \in \mathcal{E}_W \cap \mathcal{E}_{int}} \int_{\sigma} D \nabla u \cdot \mathbf{n}_{W,\sigma} v_W^n ds = 0.$$

Let us note that we consider $D \nabla u \cdot \mathbf{n}_{W,\sigma}$ in the basis $(\mathbf{n}_{W,\sigma}, \mathbf{t}_{W,\sigma})$. It means that the elements of the matrix D are given by (3.8)-(3.9). The elements of the gradient $\nabla u^n(s, t)$, in this basis are written as $\begin{pmatrix} \bar{u}_x \\ \bar{u}_y \end{pmatrix}$, are equal to $\begin{pmatrix} u_x \\ u_y \end{pmatrix}$ on right edge σ of finite volume W , $\begin{pmatrix} -u_x \\ -u_y \end{pmatrix}$ on left edge of W , $\begin{pmatrix} u_y \\ -u_x \end{pmatrix}$ on upper edge of W and $\begin{pmatrix} -u_y \\ u_x \end{pmatrix}$ on lower edge of W . The normal $\mathbf{n}_{W,\sigma}$ is equal to $\begin{pmatrix} 1 \\ 0 \end{pmatrix}$ in the basis $(\mathbf{n}_{W,\sigma}, \mathbf{t}_{W,\sigma})$ for each edge σ . Multiplying equation (3.6) by $v_W^n m(W)$ we get the discrete scheme in the form

$$(5.3) \quad \frac{(u_W^n - u_W^{n-1}) v_W^n}{k} m(W) - \sum_{\sigma \in \mathcal{E}_W \cap \mathcal{E}_{int}} \left(\bar{\lambda}_\sigma \frac{u_E^n - u_W^n}{h} + \bar{\beta}_\sigma \frac{u_N^n - u_S^n}{h} \right) m(\sigma) v_W^n = 0.$$

Then setting $v_W^n = e_W^n$ and subtracting (5.3) from (5.2) we get

$$(5.4) \quad \int_W \frac{(e_W^n - e_W^{n-1}) e_W^n}{k} dx + \sum_{\sigma \in \mathcal{E}_W \cap \mathcal{E}_{int}} \int \left[\left(\bar{\lambda}_\sigma \frac{(u_E^n - u_W^n)}{h} + \bar{\beta}_\sigma \frac{(u_N^n - u_S^n)}{h} \right) e_W^n - D\nabla u \cdot \mathbf{n}_{W,\sigma} e_W^n \right] ds = \int_W \left(\frac{u(x_W, t_n) - u(x_W, t_{n-1})}{k} - \partial_t u \right) e_W^n dx.$$

Then we sum (5.4) over $W \in \mathcal{T}_h$, integrate over (t_{n-1}, t_n) and sum again over $n = 1, \dots, m$. We apply the property $2(a-b)a = a^2 - b^2 + (a-b)^2$ to state that

$$(5.5) \quad \int_\Omega |e_{h,k}^m|^2 dx + \sum_{n=1}^m \int_\Omega |e_{h,k}^{n+1} - e_{h,k}^n|^2 dx + 2 \sum_{n=1}^m \int_{t_{n-1}}^{t_n} \sum_{\sigma \in \mathcal{E}_{int}} \int \left[\left(\bar{\lambda}_\sigma \frac{(u_E^n - u_W^n)}{h} + \bar{\beta}_\sigma \frac{(u_N^n - u_S^n)}{h} \right) e_W^n - D\nabla u \cdot \mathbf{n}_{W,\sigma} e_W^n \right] ds dt = \int_\Omega |e_{h,k}^0|^2 dx + 2 \sum_{n=1}^m \int_{t_{n-1}}^{t_n} \sum_{W \in \mathcal{T}_h} \int \left(\frac{u(x_W, t_n) - u(x_W, t_{n-1})}{k} - \partial_t u \right) e_W^n dx dt.$$

In order to rearrange the third term on the left hand side of (5.5) we define auxiliary variables Λ_{WE} and Λ_{SN} as follows

$$(5.6) \quad \Lambda_{WE} = \frac{u(x_E, t_n) - u(x_W, t_n)}{h},$$

$$(5.7) \quad \Lambda_{SN} = \sum_{\delta \in P_\sigma \cap \mathcal{E}_{int}} \frac{1}{4} \frac{u(x_{E_\delta}, t_n) - u(x_{W_\delta}, t_n)}{h}.$$

Then, using (5.6) and (5.7), we rearrange the third term into the following splitting

$$2 \sum_{n=1}^m \int_{t_{n-1}}^{t_n} \sum_{\sigma \in \mathcal{E}_{int}} \int \left[\left(\bar{\lambda}_\sigma \frac{(u_E^n - u_W^n)}{h} + \bar{\beta}_\sigma \frac{(u_N^n - u_S^n)}{h} \right) e_W^n - D\nabla u \cdot \mathbf{n}_{W,\sigma} e_W^n \right] ds dt = A_1 + A_2 + A_3 + A_4,$$

where

$$A_1 = -2 \sum_{n=1}^m \int_{t_{n-1}}^{t_n} \sum_{\sigma \in \mathcal{E}_{int}} \bar{\lambda}_\sigma \frac{(e_E^n - e_W^n)}{h} e_W^n m(\sigma) dt,$$

$$A_2 = 2 \sum_{n=1}^m \int_{t_{n-1}}^{t_n} \sum_{\sigma \in \mathcal{E}_{int}} \bar{\beta}_\sigma \left(\frac{u_N^n - u_S^n}{h} - \Lambda_{SN} \right) e_W^n m(\sigma) dt,$$

$$A_3 = 2 \sum_{n=1}^m \int_{t_{n-1}}^{t_n} \sum_{\sigma \in \mathcal{E}_{int}} \int \left((\bar{\lambda}_\sigma - \bar{\lambda}) \Lambda_{WE} + (\bar{\beta}_\sigma - \bar{\beta}) \Lambda_{SN} \right) e_W^n ds dt,$$

$$A_4 = 2 \sum_{n=1}^m \int_{t_{n-1}}^{t_n} \sum_{\sigma \in \mathcal{E}_{int}} \int_{\sigma} (\bar{\lambda} \Lambda_{WE} + \bar{\beta} \Lambda_{SN} - D \nabla u \cdot \mathbf{n}_{W,\sigma}) e_W^n ds dt,$$

where $\bar{\lambda}$ denotes $\bar{\lambda}(u)(s, t)$, $s \in \sigma$, $t \in (t_{n-1}, t_n)$ and $\bar{\lambda}_\sigma$ denotes $\bar{\lambda}(u_{h,k})(x_{WE}, t_{n-1})$, which indicates our strategy for evaluation of diffusion tensor at time t_{n-1} and in the point x_{WE} using approximation $u_{h,k}$. Owing to conservativity of numerical fluxes and fact that $m(\sigma) = h$ we have

$$A_1 = -2 \sum_{n=1}^m \int_{t_{n-1}}^{t_n} \sum_{\sigma \in \mathcal{E}_{int}} \bar{\lambda}_\sigma \frac{(e_E^n - e_W^n)}{h} e_W^n m(\sigma) dt = \sum_{n=1}^m \int_{t_{n-1}}^{t_n} \sum_{\sigma \in \mathcal{E}_{int}} \bar{\lambda}_\sigma (e_E^n - e_W^n)^2 dt.$$

Next step is to rearrange A_4 by adding and subtracting term $D \nabla u(s, t_n) \cdot \mathbf{n}_{W,\sigma}$

$$\begin{aligned} A_4 &= 2 \sum_{n=1}^m \int_{t_{n-1}}^{t_n} \sum_{\sigma \in \mathcal{E}_{int}} \int_{\sigma} (\bar{\lambda} \Lambda_{WE} + \bar{\beta} \Lambda_{SN} - D \nabla u(s, t) \cdot \mathbf{n}_{W,\sigma}) e_W^n ds dt, \\ &= 2 \sum_{n=1}^m \int_{t_{n-1}}^{t_n} \sum_{\sigma \in \mathcal{E}_{int}} \int_{\sigma} (\bar{\lambda} \Lambda_{WE} + \bar{\beta} \Lambda_{SN} - D \nabla u(s, t_n) \cdot \mathbf{n}_{W,\sigma}) e_W^n ds dt \\ &\quad + 2 \sum_{n=1}^m \int_{t_{n-1}}^{t_n} \sum_{\sigma \in \mathcal{E}_{int}} \int_{\sigma} (D \nabla u(s, t_n) - D \nabla u(s, t)) \cdot \mathbf{n}_{W,\sigma} e_W^n ds dt. \end{aligned}$$

Further, we put A_1, A_2, A_3 and A_4 into (5.5) and get

$$\begin{aligned} &\int_{\Omega} |e_{h,k}^m|^2 dx + \sum_{n=1}^m \int_{\Omega} |e_{h,k}^n - e_{h,k}^{n-1}|^2 dx + \sum_{n=1}^m \int_{t_{n-1}}^{t_n} \sum_{\sigma \in \mathcal{E}_{int}} \bar{\lambda}_\sigma (e_E^n - e_W^n)^2 dt \\ (5.8) \quad &= \int_{\Omega} |e_{h,k}^0|^2 dx + B_1 + B_2 + B_3 + B_4 + B_5 + B_6, \end{aligned}$$

where

$$\begin{aligned} B_1 &= 2 \sum_{n=1}^m \int_{t_{n-1}}^{t_n} \sum_{W \in \mathcal{T}_h} \int_W \left(\frac{u(x_W, t_n) - u(x_W, t_{n-1})}{k} - \partial_t u \right) e_W^n dx dt, \\ B_2 &= -2 \sum_{n=1}^m \int_{t_{n-1}}^{t_n} \sum_{\sigma \in \mathcal{E}_{int}} \bar{\beta}_\sigma \left(\frac{u_N^n - u_S^n}{h} - \Lambda_{SN} \right) e_W^n m(\sigma) dt, \\ B_3 &= -2 \sum_{n=1}^m \int_{t_{n-1}}^{t_n} \sum_{\sigma \in \mathcal{E}_{int}} \int_{\sigma} (\bar{\lambda}_\sigma - \bar{\lambda}) \Lambda_{WE} e_W^n ds dt, \\ B_4 &= -2 \sum_{n=1}^m \int_{t_{n-1}}^{t_n} \sum_{\sigma \in \mathcal{E}_{int}} \int_{\sigma} (\bar{\beta}_\sigma - \bar{\beta}) \Lambda_{SN} e_W^n ds dt, \end{aligned}$$

$$B_5 = -2 \sum_{n=1}^m \int_{t_{n-1}}^{t_n} \sum_{\sigma \in \mathcal{E}_{int} \sigma} \int (\bar{\lambda} \Lambda_{WE} + \bar{\beta} \Lambda_{SN} - D\nabla u(s, t_n) \cdot \mathbf{n}_{W, \sigma}) e_W^n ds dt,$$

$$B_6 = -2 \sum_{n=1}^m \int_{t_{n-1}}^{t_n} \sum_{\sigma \in \mathcal{E}_{int} \sigma} \int (D\nabla u(s, t_n) - D\nabla u(s, t)) \cdot \mathbf{n}_{W, \sigma} e_W^n ds dt.$$

Now we bound each term B_i , $i = 1, 2, \dots, 6$ and begin with B_1 , where we can estimate

$$\left| \frac{u(x_W, t_n) - u(x_W, t_{n-1})}{k} - \partial_t u \right| \leq \frac{1}{k} \left| \int_{t_{n-1}}^{t_n} \int_0^1 \nabla u_t(x + z(x_W - x), g) \cdot (x_W - x) dz dg \right| + \left| \int_{t_{n-1}}^{t_n} u_{tt}(x, g) dg \right|.$$

Applying previous inequality we have

$$|B_1| \leq 2 \sum_{n=1}^m \int_{t_{n-1}}^{t_n} \sum_{W \in \mathcal{T}_h W} \int \left(\frac{h}{k} \int_{t_{n-1}}^{t_n} \int_0^1 |\nabla u_t(x_W + z(x_W - x), g)| dz dg + \int_{t_{n-1}}^{t_n} |u_{tt}(x, g)| dg \right) |e_W^n| dx dt.$$

Then we use Young's inequality to obtain

$$|B_1| \leq \sum_{n=1}^m \int_{t_{n-1}}^{t_n} \sum_{W \in \mathcal{T}_h W} \int (e_W^n)^2 dx dt + \sum_{n=1}^m \int_{t_{n-1}}^{t_n} \sum_{W \in \mathcal{T}_h W} \int \left(\frac{h}{k} \int_{t_{n-1}}^{t_n} \int_0^1 |\nabla u_t(x_W + z(x_W - x), g)| dz dg + \int_{t_{n-1}}^{t_n} |u_{tt}(x, g)| dg \right)^2 dx dt,$$

and from it we get

$$(5.9) \quad |B_1| \leq 2k^2 \|u_{tt}\|_{L_2(I, L_2(\Omega))}^2 + 2h^2 \|\nabla u_t\|_{L_2(I, L_2(\Omega))}^2 + \sum_{n=0}^{m-1} \int_{t_{n-1}}^{t_n} \int_{\Omega} |e_{h,k}^n|^2 dx dt.$$

Concerning the second term we can write

$$\begin{aligned} B_2 &= - \sum_{n=1}^m \int_{t_{n-1}}^{t_n} \sum_{\sigma \in \mathcal{E}_{int} \sigma} \frac{\bar{\beta}_\sigma}{2} \sum_{\delta \in P_\sigma \cap \mathcal{E}_{int} \sigma} \left(\frac{u_{E_\delta} - u_{W_\delta}}{h} - \frac{u(x_{E_\delta}, t_n) - u(x_{W_\delta}, t_n)}{h} \right) e_W^n m(\sigma) dt \\ &= \sum_{n=1}^m \int_{t_{n-1}}^{t_n} \sum_{\sigma \in \mathcal{E}_{int} \sigma} \frac{\bar{\beta}_\sigma}{2\sqrt{\bar{\lambda}_\sigma}} \sum_{\delta \in P_\sigma \cap \mathcal{E}_{int} \sigma} \frac{(e_{E_\delta}^n - e_{W_\delta}^n)}{h} \sqrt{\bar{\lambda}_\sigma} e_W^n m(\sigma) dt \\ &= \frac{1}{2} \sum_{n=1}^m \int_{t_{n-1}}^{t_n} \sum_{\sigma \in \mathcal{E}_{int} \sigma} \frac{\bar{\beta}_\sigma}{2\sqrt{\bar{\lambda}_\sigma}} \sum_{\delta \in P_\sigma \cap \mathcal{E}_{int} \sigma} \frac{(e_{E_\delta}^n - e_{W_\delta}^n)}{h} \sqrt{\bar{\lambda}_\sigma} (e_W^n - e_E^n) m(\sigma) dt \\ &\leq \frac{1}{4} \sum_{n=1}^m \int_{t_{n-1}}^{t_n} \sum_{\sigma \in \mathcal{E}_{int} \sigma} \bar{\lambda}_\sigma \frac{(e_E^n - e_W^n)^2}{h} m(\sigma) dt \end{aligned}$$

$$+ \frac{1}{4} \sum_{n=1}^m \int_{t_{n-1}}^{t_n} \sum_{\sigma \in \mathcal{E}_{int}} \frac{\bar{\beta}_\sigma^2}{2\bar{\lambda}_\sigma} \sum_{\delta \in P_\sigma \cap \mathcal{E}_{int}} \frac{(e_{E_\delta}^n - e_{W_\delta}^n)^2}{h^2} hm(\sigma) dt.$$

Similarly to the proof of (4.1), given in section 3 of [4], we get

$$\sum_{\sigma \in \mathcal{E}_{int}} \left(\frac{\bar{\beta}_\sigma}{\bar{\lambda}_\sigma} \right)^2 \sum_{\delta \in P_\sigma \cap \mathcal{E}_{int}} \frac{1}{4} \left(\frac{e_{E_\delta}^n - e_{W_\delta}^n}{h} \right)^2 \bar{\lambda}_\sigma \leq \gamma \sum_{\sigma \in \mathcal{E}_{int}} \left(\frac{e_E^n - e_W^n}{h} \right)^2 \bar{\lambda}_\sigma$$

with γ given in (4.1). Then we have

$$B_2 \leq \frac{1}{4} \sum_{n=1}^m \int_{t_{n-1}}^{t_n} \sum_{\sigma \in \mathcal{E}_{int}} \bar{\lambda}_\sigma (e_E^n - e_W^n)^2 dt + \frac{\gamma}{2} \sum_{n=1}^m \int_{t_{n-1}}^{t_n} \sum_{\sigma \in \mathcal{E}_{int}} \bar{\lambda}_\sigma (e_E^n - e_W^n)^2 dt,$$

which yields

$$(5.10) \quad B_2 \leq \frac{1+2\gamma}{4} \sum_{n=1}^m \int_{t_{n-1}}^{t_n} \sum_{\sigma \in \mathcal{E}_{int}} \bar{\lambda}_\sigma (e_E^n - e_W^n)^2 dt.$$

Let us rewrite term B_3 as

$$B_3 = \sum_{n=1}^m \int_{t_{n-1}}^{t_n} \sum_{\sigma \in \mathcal{E}_{int}} \int_{\sigma} (\bar{\lambda}_\sigma - \bar{\lambda}) \frac{(u(x_E, t_n) - u(x_W, t_n))}{h} (e_E^n - e_W^n) ds dt.$$

Thanks to regularity of the solution u we know that

$$|B_3| \leq \|\nabla u\|_{L^\infty(Q_T)} \sum_{n=1}^m \int_{t_{n-1}}^{t_n} \sum_{\sigma \in \mathcal{E}_{int}} \int_{\sigma} |\bar{\lambda}_\sigma - \bar{\lambda}| |e_E^n - e_W^n| ds dt.$$

Using Young's inequality we obtain

$$|B_3| \leq B_{3A} + B_{3B},$$

where

$$(5.11) \quad B_{3A} = \frac{\omega}{2} \sum_{n=1}^m k \sum_{\sigma \in \mathcal{E}_{int}} \bar{\lambda}_\sigma \frac{(e_E^n - e_W^n)^2}{h} m(\sigma) = \frac{\omega}{2} \sum_{n=1}^m k \sum_{\sigma \in \mathcal{E}_{int}} \bar{\lambda}_\sigma (e_E^n - e_W^n)^2,$$

$$(5.12) \quad B_{3B} = \frac{1}{2\omega} \|\nabla u\|_{L^\infty(Q_T)}^2 \sum_{n=1}^m \int_{t_{n-1}}^{t_n} \sum_{\sigma \in \mathcal{E}_{int}} \int_{\sigma} \frac{(\bar{\lambda}_\sigma - \bar{\lambda})^2}{\bar{\lambda}_\sigma} h ds dt$$

and ω is a sufficiently small parameter. Our notation $\bar{\lambda}_\sigma - \bar{\lambda}$ means rigorously $\bar{\lambda}(u_{h,k})(x_{WE}, t_{n-1}) - \bar{\lambda}(u)(s, t)$. In order to estimate this difference we introduce the following lemma, which gives an estimate between elements of discrete and exact diffusion tensor. Let us note that the construction of D_σ and D described by (2.4)-(2.8) is the same, the index σ is used only because the tensor D_σ is evaluated using numerical solution on edge σ , and the arguments are different. In the first case it is

the numerical solution $u_{h,k}$, which is used in evaluation of diffusion tensor at point $x_{WE} \in \sigma$ and at time t_{n-1} , where x_{WE} is a point of $\sigma_{WE} = W|E$ intersecting the segment $x_W x_E$. In the second case the argument is given by the function u and the tensor is evaluated at any point $s \in \sigma$ and $t \in (t_{n-1}, t_n)$.

LEMMA 5.2. *There exist a positive constant C such that*

$$(5.13) \quad \begin{aligned} & |\bar{\lambda}(u_{h,k})(x_{WE}, t_{n-1}) - \bar{\lambda}(u)(s, t)| \leq C(h + \|u_{h,k}(t-k) - u_{h,k}(t)\|_{L_2(\Omega)} \\ & \quad + \|u_{h,k}(t) - u(t)\|_{L_2(\Omega)} + \|u(t)\|_{L_2(\Omega)} \|u(t) - u_{h,k}(t)\|_{L_2(\Omega)}). \end{aligned}$$

and

$$(5.14) \quad \begin{aligned} & |\bar{\beta}(u_{h,k})(x_{WE}, t_{n-1}) - \bar{\beta}(u)(s, t)| \leq C(h + \|u_{h,k}(t-k) - u_{h,k}(t)\|_{L_2(\Omega)} \\ & \quad + \|u_{h,k}(t) - u(t)\|_{L_2(\Omega)} + \|u(t)\|_{L_2(\Omega)} \|u(t) - u_{h,k}(t)\|_{L_2(\Omega)}). \end{aligned}$$

Proof. The basic ingredients of the proof are given by the properties of functions $\bar{\lambda}$ and $\bar{\beta}$ as Lipschitz functions of the partial derivatives of solution (smoothed by spatial convolutions). We show the Lipschitz continuity for all functions λ, β, ν , because $\bar{\lambda}$ and $\bar{\beta}$ may be equal to one of them, cf. (3.8)-(3.9), depending on the local basis in which both matrices D_σ and D are written. From the diffusion tensor construction, cf. (2.4)-(2.8), it follows that we can write the estimated terms in the following form,

$$(5.15) \quad |\bar{\lambda}(a_{h,k}^{n-1}, b_{h,k}^{n-1}, c_{h,k}^{n-1}) - \bar{\lambda}(a, b, c)| \quad \text{or} \quad |\bar{\beta}(a_{h,k}^{n-1}, b_{h,k}^{n-1}, c_{h,k}^{n-1}) - \bar{\beta}(a, b, c)|,$$

where

$$\begin{aligned} a &= \left(G_\rho * \left(\frac{\partial G_{\bar{t}}}{\partial x} * u \right)^2 \right) (s, t), \\ b &= \left(G_\rho * \left[\left(\frac{\partial G_{\bar{t}}}{\partial x} * u \right) \left(\frac{\partial G_{\bar{t}}}{\partial y} * u \right) \right] \right) (s, t), \\ c &= \left(G_\rho * \left(\frac{\partial G_{\bar{t}}}{\partial y} * u \right)^2 \right) (s, t), \\ a_{h,k}^{n-1} &= \left(G_\rho * \left(\frac{\partial G_{\bar{t}}}{\partial x} * u_{h,k} \right)^2 \right) (x_{WE}, t_{n-1}), \\ b_{h,k}^{n-1} &= \left(G_\rho * \left[\left(\frac{\partial G_{\bar{t}}}{\partial x} * u_{h,k} \right) \left(\frac{\partial G_{\bar{t}}}{\partial y} * u_{h,k} \right) \right] \right) (x_{WE}, t_{n-1}), \\ c_{h,k}^{n-1} &= \left(G_\rho * \left(\frac{\partial G_{\bar{t}}}{\partial y} * u_{h,k} \right)^2 \right) (x_{WE}, t_{n-1}) \end{aligned}$$

and $\bar{\lambda}, \bar{\beta}$ is equal to one of the functions λ, β, ν depending on the above defined three arguments as follows

$$\begin{aligned} \lambda(a, b, c) &= \frac{\kappa_1 v_1^2 + \kappa_2 v_2^2}{v_1^2 + v_2^2} = \\ &= \begin{cases} \alpha, & \text{if } \mu_1 = \mu_2 \text{ (i.e. if } \sqrt{4b^2 + (a-c)^2} = 0), \\ \alpha + (1-\alpha) \left(\frac{1}{2} + \frac{c-a}{2\sqrt{4b^2 + (a-c)^2}} \right) e^{-\frac{1}{4b^2 + (a-c)^2}}, & \text{else.} \end{cases} \end{aligned}$$

$$\begin{aligned}
\beta(a, b, c) &= \frac{v_1 v_2 (\kappa_1 - \kappa_2)}{v_1^2 + v_2^2} = \\
&= \begin{cases} 0, & \text{if } \mu_1 = \mu_2 \text{ (i.e. if } \sqrt{4b^2 + (a-c)^2} = 0), \\ \frac{(\alpha-1)b}{\sqrt{4b^2 + (a-c)^2}} e^{-\frac{1}{4b^2 + (a-c)^2}}, & \text{else.} \end{cases} \\
\nu(a, b, c) &= \frac{\kappa_2 v_1^2 + \kappa_1 v_2^2}{v_1^2 + v_2^2} = \\
&= \begin{cases} \alpha, & \text{if } \mu_1 = \mu_2 \text{ (i.e. if } \sqrt{4b^2 + (a-c)^2} = 0), \\ \alpha + (1-\alpha) \left(\frac{1}{2} - \frac{c-a}{2\sqrt{4b^2 + (a-c)^2}} \right) e^{-\frac{1}{4b^2 + (a-c)^2}}, & \text{else.} \end{cases}
\end{aligned}$$

If we denote by $F = 4b^2 + (a-c)^2$ the values of λ, β, ν for $F = 0$ are defined as limit values as $F \rightarrow 0$ and thus the functions are continuous.

From such form of λ, β, ν one can simply see that they are uniformly bounded. We can write

$$\lambda(a, b, c) = \alpha + (1-\alpha) \left(\frac{1}{2} + \frac{c-a}{2\sqrt{F}} \right) e^{-\frac{1}{F}}.$$

Since $|a-c| \leq \sqrt{4b^2 + (a-c)^2} = \sqrt{F}$ and $\alpha \in (0, 1)$, we get

$$(5.16) \quad |\lambda| \leq \alpha + (1-\alpha) \left(\frac{1}{2} + \frac{\sqrt{F}}{2\sqrt{F}} \right) e^{-\frac{1}{F}} \leq 1.$$

and similarly for β and ν .

From the structure of λ, β, ν we can also see that their partial derivatives of any order, with respect to a, b, c will contain a product of the term $e^{-\frac{1}{F}}$ and a rational polynomial, which can be estimated by powers of F , and which together give uniform bounds on the derivatives. In our proof it is sufficient to have Lipschitz continuity of λ, β, ν , so we show that their first partial derivatives are uniformly bounded. First we have

$$\frac{\partial \lambda}{\partial a} = (1-\alpha)(a-c) \frac{e^{-\frac{1}{F}}}{F^2} + (\alpha-1)(8b^4 + 2b^2(a-c)^2 + (a-c)^2) \frac{e^{-\frac{1}{F}}}{F^{\frac{5}{2}}}.$$

Since $|\alpha| < 1$, $|1-\alpha| < 1$ and $|a-c| \leq F^{\frac{1}{2}}$ we have

$$\begin{aligned}
\left| \frac{\partial \lambda}{\partial a} \right| &\leq |a-c| \frac{e^{-\frac{1}{F}}}{F^2} + ((4b^2 + (a-c)^2)^2 + (a-c)^2 + 4b^2) \frac{e^{-\frac{1}{F}}}{F^{\frac{5}{2}}} \\
&\leq \frac{F e^{-\frac{1}{F}}}{F^{\frac{5}{2}}} + \frac{(F^2 + F) e^{-\frac{1}{F}}}{F^{\frac{5}{2}}} = \frac{F+2}{F^{\frac{3}{2}}} e^{-\frac{1}{F}} = h_1(F) \leq \max_{F \geq 0} h_1(F) = h_1(F_1),
\end{aligned}$$

where $F_1 = 2(\sqrt{2}-1)$, so

$$(5.17) \quad \left| \frac{\partial \lambda}{\partial a} \right| \leq C_1 \leq 1.2.$$

Then we similarly get

$$\frac{\partial \lambda}{\partial b} = (1-\alpha) \frac{4be^{-\frac{1}{F}}}{F^2} + (1-\alpha) 2b(a-c)(4b^2 + (a-c)^2 - 2) \frac{e^{-\frac{1}{F}}}{F^{\frac{5}{2}}}.$$

Since $2|b| \leq \sqrt{4b^2 + (a-c)^2} = F^{\frac{1}{2}}$ we have

$$\begin{aligned} \left| \frac{\partial \lambda}{\partial b} \right| &\leq \frac{2F^{\frac{1}{2}}e^{-\frac{1}{F}}}{F^2} + \frac{F^{\frac{1}{2}}F^{\frac{1}{2}}(F+2)e^{-\frac{1}{F}}}{F^{\frac{5}{2}}} = \frac{(F+4)e^{-\frac{1}{F}}}{F^{\frac{3}{2}}} \\ &= h_2(F) \leq \max_{F \geq 0} h_2(F) = h_2(F_2), \end{aligned}$$

where $F_2 = \sqrt{33} - 5$, so

$$(5.18) \quad \left| \frac{\partial \lambda}{\partial b} \right| \leq C_2 \leq 2.$$

Since

$$\frac{\partial \lambda}{\partial c} = (\alpha - 1)(a - c) \frac{e^{-\frac{1}{F}}}{F^2} + (1 - \alpha)(8b^4 + 2b^2(a - c)^2 + (a - c)^2) \frac{e^{-\frac{1}{F}}}{F^{\frac{5}{2}}} = -\frac{\partial \lambda}{\partial a}$$

we get

$$(5.19) \quad \left| \frac{\partial \lambda}{\partial c} \right| = \left| \frac{\partial \lambda}{\partial a} \right| \leq C_1.$$

For the function ν we get

$$\frac{\partial \nu}{\partial a} = (1 - \alpha)(a - c) \frac{e^{-\frac{1}{F}}}{F^2} + (1 - \alpha)(8b^4 + 2b^2(a - c)^2 + (a - c)^2) \frac{e^{-\frac{1}{F}}}{F^{\frac{5}{2}}}$$

so we get the same estimate as in (5.17) and (5.19) also for $\left| \frac{\partial \nu}{\partial a} \right|$. Since

$$\frac{\partial \nu}{\partial b} = (1 - \alpha) \frac{4be^{-\frac{1}{F}}}{F^2} + (\alpha - 1)2b(a - c)(4b^2 + (a - c)^2 - 2) \frac{e^{-\frac{1}{F}}}{F^{\frac{5}{2}}},$$

so we get the same estimate as in (5.18) for $\left| \frac{\partial \nu}{\partial b} \right|$, and because $\frac{\partial \nu}{\partial c} = -\frac{\partial \nu}{\partial a}$ we have again $\left| \frac{\partial \nu}{\partial c} \right| \leq C_1$. For the function β we have

$$\frac{\partial \beta}{\partial a} = (1 - \alpha)b(a - c)(4b^2 + (a - c)^2 - 2) \frac{e^{-\frac{1}{F}}}{F^{\frac{5}{2}}},$$

thus

$$\left| \frac{\partial \beta}{\partial a} \right| \leq \frac{F^{\frac{1}{2}}F^{\frac{1}{2}}(F+2)e^{-\frac{1}{F}}}{F^{\frac{5}{2}}} = \frac{(F+2)e^{-\frac{1}{F}}}{F^{\frac{3}{2}}} \leq h_1(F_1)$$

and therefore

$$(5.20) \quad \left| \frac{\partial \beta}{\partial a} \right| \leq C_1.$$

We also have

$$\frac{\partial \beta}{\partial b} = (\alpha - 1)(8b^2 + 4b^2(a - c)^2 + (a - c)^4) \frac{e^{-\frac{1}{F}}}{F^{\frac{5}{2}}},$$

so

$$\left| \frac{\partial \beta}{\partial b} \right| \leq (2(4b^2 + (a - c)^2) + (4b^2 + (a - c)^2)^2) \frac{e^{-\frac{1}{F}}}{F^{\frac{5}{2}}} = \frac{2F + F^2}{F^{\frac{5}{2}}} e^{-\frac{1}{F}} \leq h_1(F_1)$$

and from it $\left| \frac{\partial \beta}{\partial b} \right| \leq C_1$. Using $\frac{\partial \beta}{\partial c} = -\frac{\partial \beta}{\partial a}$ we also get $\left| \frac{\partial \beta}{\partial c} \right| \leq C_1$.

The relation in (5.15) contains differences of either λ , β or ν evaluated in different arguments. Using boundedness of their partial derivatives, and thus the Lipschitz continuity, those differences can be estimated by the differences of the arguments. We will do it only for λ , all other situations are treated similarly. We have

$$(5.21) \quad \begin{aligned} |\lambda(a_{h,k}^{n-1}, b_{h,k}^{n-1}, c_{h,k}^{n-1}) - \lambda(a, b, c)| &\leq L_\lambda \sqrt{(a_{h,k}^{n-1} - a)^2 + (b_{h,k}^{n-1} - b)^2 + (c_{h,k}^{n-1} - c)^2} \\ &\leq L_\lambda (|a_{h,k}^{n-1} - a| + |b_{h,k}^{n-1} - b| + |c_{h,k}^{n-1} - c|), \end{aligned}$$

where L_λ is the Lipschitz constant of function λ . Since all terms in the absolute values on the right hand side of (5.21) can be estimated similarly, we do it in details just for the first one $|a_{h,k}^{n-1} - a|$. A slight difference is only when treating $|b_{h,k}^{n-1} - b|$ and we will also mention it later. We can use the following splitting and get

$$\begin{aligned} |a_{h,k}^{n-1} - a| &\leq \left| \left(G_\rho * \left(\frac{\partial G_{\bar{t}}}{\partial x} * u_{h,k} \right)^2 \right) (x_{WE}, t_{n-1}) - \left(G_\rho * \left(\frac{\partial G_{\bar{t}}}{\partial x} * u_{h,k} \right)^2 \right) (s, t_{n-1}) \right| \\ &\quad + \left| \left(G_\rho * \left(\frac{\partial G_{\bar{t}}}{\partial x} * u_{h,k} \right)^2 \right) (s, t_{n-1}) - \left(G_\rho * \left(\frac{\partial G_{\bar{t}}}{\partial x} * u_{h,k} \right)^2 \right) (s, t) \right| \\ &\quad + \left| \left(G_\rho * \left(\frac{\partial G_{\bar{t}}}{\partial x} * u_{h,k} \right)^2 \right) (s, t) - \left(G_\rho * \left(\frac{\partial G_{\bar{t}}}{\partial x} * u \right)^2 \right) (s, t) \right| \\ &= J_1 + J_2 + J_3. \end{aligned}$$

Then subsequently

$$\begin{aligned} J_1 &\leq \left| \int_{R^N} G_\rho(x_{WE} - \xi) \left(\int_{R^N} \frac{\partial G_{\bar{t}}}{\partial x}(\xi - \eta) u_{h,k}(\eta, t_{n-1}) d\eta \right)^2 d\xi - \right. \\ &\quad \left. - \int_{R^N} G_\rho(s - \xi) \left(\int_{R^N} \frac{\partial G_{\bar{t}}}{\partial x}(\xi - \eta) u_{h,k}(\eta, t_{n-1}) d\eta \right)^2 d\xi \right| \leq \\ &\leq \int_{R^N} |G_\rho(x_{WE} - \xi) - G_\rho(s - \xi)| \left(\int_{R^N} \frac{\partial G_{\bar{t}}}{\partial x}(\xi - \eta) u_{h,k}(\eta, t_{n-1}) d\eta \right)^2 d\xi \leq Ch, \end{aligned}$$

because of the fact that $|x_{WE} - s| \leq h$, C^∞ smoothness of G_ρ and because

$$\begin{aligned} \left(\int_{R^N} \frac{\partial G_{\bar{t}}}{\partial x}(\xi - \eta) u_{h,k}(\eta, t_{n-1}) d\eta \right)^2 &\leq C \int_{R^N} \left(\frac{\partial G_{\bar{t}}}{\partial x}(\xi - \eta) \right)^2 d\eta \int_{\Omega} u_{h,k}^2(\eta, t_{n-1}) d\eta \leq \\ &\leq C \|u_{h,k}(t_{n-1})\|_{L_2(\Omega)}^2 \leq C \end{aligned}$$

holds for any $\xi \in R^N$, using the Cauchy-Schwarz inequality, C^∞ smoothness of $G_{\bar{t}}$ and extension by 0 of $u_{h,k}$ outside a neighbourhood of Ω .

The second term can be written as follows

$$J_2 = \int_{R^N} G_\rho(s - \xi) \left[\left(\int_{R^N} \frac{\partial G_{\bar{t}}}{\partial x}(\xi - \eta) u_{h,k}(\eta, t_{n-1}) d\eta \right)^2 \right]$$

$$- \left(\int_{\mathbb{R}^N} \frac{\partial G_{\bar{t}}}{\partial x}(\xi - \eta) u_{h,k}(\eta, t) d\eta \right)^2 \Big] d\xi = \int_{\mathbb{R}^N} G_\rho(s - \xi) K_1 d\xi,$$

and for the term K_1 , using the relation $|p^2 - q^2| = |p+q||p-q|$, we get for any $\xi \in \mathbb{R}^N$, $t \in (t_{n-1}, t_n)$ that

$$\begin{aligned} |K_1| &= \left| \int_{\mathbb{R}^N} \frac{\partial G_{\bar{t}}}{\partial x}(\xi - \eta) (u_{h,k}(\eta, t_{n-1}) + u_{h,k}(\eta, t)) d\eta \right| \cdot \left| \int_{\mathbb{R}^N} \frac{\partial G_{\bar{t}}}{\partial x}(\xi - \eta) (u_{h,k}(\eta, t_{n-1}) - u_{h,k}(\eta, t)) d\eta \right| \\ &\leq C (\|u_{h,k}(\eta, t_{n-1})\|_{L_2(\Omega)} + \|u_{h,k}(\eta, t)\|_{L_2(\Omega)}) \|u_{h,k}(t-k) - u_{h,k}(t)\|_{L_2(\Omega)} \\ &\leq C \|u_{h,k}(t-k) - u_{h,k}(t)\|_{L_2(\Omega)}, \end{aligned}$$

where the Cauchy-Schwarz inequality and piecewise constant in time definition of $u_{h,k}$ was used. Then also

$$|J_2| \leq C \|u_{h,k}(t-k) - u_{h,k}(t)\|_{L_2(\Omega)}$$

because $\int_{\mathbb{R}^N} G_\rho(s - \xi) d\xi = 1$ for any s .

For the third term we have

$$\begin{aligned} J_3 &= \left| \int_{\mathbb{R}^N} G_\rho(s - \xi) \left[\left(\int_{\mathbb{R}^N} \frac{\partial G_{\bar{t}}}{\partial x}(\xi - \eta) u_{h,k}(\eta, t) d\eta \right)^2 - \left(\int_{\mathbb{R}^N} \frac{\partial G_{\bar{t}}}{\partial x}(\xi - \eta) u(\eta, t) d\eta \right)^2 \right] d\xi \right| \\ &= \left| \int_{\mathbb{R}^N} G_\rho(s - \xi) K_2 d\xi \right| \end{aligned}$$

and again due to the Cauchy-Schwarz inequality we get

$$\begin{aligned} |K_2| &= \left| \int_{\mathbb{R}^N} \frac{\partial G_{\bar{t}}}{\partial x}(\xi - \eta) (u_{h,k}(\eta, t) + u(\eta, t)) d\eta \right| \left| \int_{\mathbb{R}^N} \frac{\partial G_{\bar{t}}}{\partial x}(\xi - \eta) (u_{h,k}(\eta, t) - u(\eta, t)) d\eta \right| \\ &\leq C \|u_{h,k}(t) - u(t)\|_{L_2(\Omega)} + C \|u(t)\|_{L_2(\Omega)} \|u_{h,k}(t) - u(t)\|_{L_2(\Omega)}. \end{aligned}$$

and so

$$|J_3| \leq C \|u_{h,k}(t) - u(t)\|_{L_2(\Omega)} + C \|u(t)\|_{L_2(\Omega)} \|u_{h,k}(t) - u(t)\|_{L_2(\Omega)}.$$

Let us note that for $|b_{h,k}^{n-1} - b|$ we can use the same approach as above, but in the terms which would correspond to J_2 and J_3 , we would use $|p_1 q_1 - p_2 q_2| \leq |p_1(q_1 - q_2)| + |(p_1 - p_2)q_2|$ in order to get the same estimates as above. For the term $|c_{h,k}^{n-1} - c|$ we can use completely same approach as above. Putting together all previous estimates we end the proof of Lemma 5.2. \square

Next we also show that

$$\bar{\lambda}_\sigma \geq C > 0, \text{ for all } \sigma \in \mathcal{E}_{int}.$$

The matrices B and D , cf. (2.8), are similar and positive definite. We can write for their traces

$$(5.22) \quad Tr(D) = Tr(B) = \kappa_1 + \kappa_2 \in [2\alpha, \alpha + 1].$$

Thanks to (5.22), we have $\bar{\nu}_\sigma < Tr(D) \leq \alpha + 1$. The use of determinants leads to $\bar{\lambda}_\sigma \bar{\nu}_\sigma - \bar{\beta}_\sigma^2 = |D| = |B| = \kappa_1 \kappa_2 \geq \alpha^2$, and from it $\bar{\lambda}_\sigma > \frac{\alpha^2}{\bar{\nu}_\sigma} > \frac{\alpha^2}{\alpha+1} = C$.

It comes from regularity of the solution, boundedness of $\bar{\lambda}_\sigma$ and application of the Cauchy-Schwarz inequality that

$$B_{3B} \leq C(\omega)h \sum_{n=1}^m \int_{t_{n-1}}^{t_n} \sum_{\sigma \in \mathcal{E}_{int}} \int_{\sigma} (\bar{\lambda}_\sigma - \bar{\lambda})^2 ds dt.$$

Lemma 5.2, regularity of u and inequality $(a+b)^2 \leq 2a^2 + 2b^2$ lead to

$$(5.23) \quad |B_{3B}| \leq 4C(\omega)h^2 \sum_{n=1}^m \int_{t_{n-1}}^{t_n} \sum_{\sigma \in \mathcal{E}_{int}} (h^2 + \|u_{h,k}(x, t-k) - u_{h,k}(x, t)\|_{L_2(\Omega)}^2 + \|u_{h,k}(x, t) - u(x, t)\|_{L_2(\Omega)}^2) dt.$$

Owing to geometrical arguments, we know that

$$\sum_{\sigma \in \mathcal{E}_{int}} d_{WE} m(\sigma) = C|\Omega|,$$

which yields

$$(5.24) \quad \sum_{\sigma \in \mathcal{E}_{int}} h^2 = C|\Omega|$$

for our uniform square mesh. Now, we estimate each term on the right hand side of (5.23). Thanks to relation (5.24) we simply bound the first term as follows

$$(5.25) \quad C(\omega)h^2 \sum_{n=1}^m \int_{t_{n-1}}^{t_n} \sum_{\sigma \in \mathcal{E}_{int}} h^2 dt \leq C(\omega)|\Omega|Th^2.$$

The second term can be rewritten again using the relation (5.24) in the form

$$(5.26) \quad \begin{aligned} & C(\omega) \sum_{n=1}^m \int_{t_{n-1}}^{t_n} \|u_{h,k}(x, t-k) - u_{h,k}(x, t)\|_{L_2(\Omega)}^2 \sum_{\sigma \in \mathcal{E}_{int}} h^2 dt \\ & \leq C(\omega)|\Omega| \int_0^T \int_{\Omega} (u_{h,k}(x, t-k) - u_{h,k}(x, t))^2 dx dt \leq C(\omega)k \end{aligned}$$

due to the time translate estimate, cf. Lemma 4.5. We treat the third term in the similar way as previous one and obtain

$$C(\omega) \sum_{n=1}^m \int_{t_{n-1}}^{t_n} \|u_{h,k}(x, t) - u(x, t)\|_{L_2(\Omega)}^2 \sum_{\sigma \in \mathcal{E}_{int}} h^2 dt$$

$$\begin{aligned}
&\leq C(\omega)|\Omega| \int_0^T \int_{\Omega} (u_{h,k}(x,t) - u(x,t))^2 dx dt = C(\omega) \|u_{h,k}(x,t) - u(x,t)\|_{L_2(Q_T)}^2 \\
(5.27) \quad &= C(\omega) \|e_{h,k}(x,t)\|_{L_2(Q_T)}^2 = C(\omega) \sum_{n=1}^m \int_{t_{n-1}}^{t_n} \int_{\Omega} |e_{h,k}^n|^2 dx dt.
\end{aligned}$$

Finally, applying (5.25), (5.26) and (5.27) in (5.23) we get

$$|B_{3B}| \leq C(\omega)Th^2 + C(\omega)k + C(\omega) \sum_{n=1}^m \int_{t_{n-1}}^{t_n} \int_{\Omega} |e_{h,k}^n|^2 dx dt,$$

which together with (5.11) result in

$$\begin{aligned}
|B_3| &\leq \frac{\omega}{2} \sum_{n=1}^m k \sum_{\sigma \in \mathcal{E}_{int}} \bar{\lambda}_{\sigma} (e_W^n - e_E^n)^2 \\
(5.28) \quad &+ C(\omega)Th^2 + C(\omega)k + C(\omega) \sum_{n=1}^m \int_{t_{n-1}}^{t_n} \int_{\Omega} |e_{h,k}^n|^2 dx dt.
\end{aligned}$$

Using the same tricks as for the term B_3 we can state that

$$\begin{aligned}
|B_4| &\leq \frac{\omega}{2} \sum_{n=1}^m k \sum_{\sigma \in \mathcal{E}_{int}} \bar{\lambda}_{\sigma} (e_W^n - e_E^n)^2 \\
(5.29) \quad &+ C(\omega)Th^2 + C(\omega)k + C(\omega) \sum_{n=1}^m \int_{t_{n-1}}^{t_n} \int_{\Omega} |e_{h,k}^n|^2 dx dt.
\end{aligned}$$

As usual in finite volume methods, we rearrange the term B_5 in the form

$$\begin{aligned}
B_5 &= -2 \sum_{n=1}^m \int_{t_{n-1}}^{t_n} \sum_{\sigma \in \mathcal{E}_{int}} \int_{\sigma} (\bar{\lambda}\Lambda_{WE} + \bar{\beta}\Lambda_{SN} - D\nabla u(s, t_n) \cdot \mathbf{n}_{W,\sigma}) e_W^n ds dt \\
&= \sum_{n=1}^m \int_{t_{n-1}}^{t_n} \sum_{\sigma \in \mathcal{E}_{int}} \int_{\sigma} (\bar{\lambda}\Lambda_{WE} + \bar{\beta}\Lambda_{SN} - D\nabla u(s, t_n) \cdot \mathbf{n}_{W,\sigma}) (e_E^n - e_W^n) ds dt \\
&= \sum_{n=1}^m \int_{t_{n-1}}^{t_n} \sum_{\sigma \in \mathcal{E}_{int}} m(\sigma) \left(\bar{\lambda}\Lambda_{WE} + \bar{\beta}\Lambda_{SN} - \frac{1}{m(\sigma)} \int_{\sigma} D\nabla u(s, t_n) \cdot \mathbf{n}_{W,\sigma} ds \right) (e_E^n - e_W^n) dt.
\end{aligned}$$

Next step is to define an auxiliary unknown B_{5A} by

$$B_{5A} = \bar{\lambda}\Lambda_{WE} + \bar{\beta}\Lambda_{SN} - \frac{1}{m(\sigma)} \int_{\sigma} D\nabla u(s, t_n) \cdot \mathbf{n}_{W,\sigma} ds.$$

Then we can write

$$|B_{5A}| \leq \left| \bar{\lambda} \left(\Lambda_{WE} - \frac{1}{m(\sigma)} \int_{\sigma} \bar{u}_x(s, t_n) ds \right) + \bar{\beta} \left(\Lambda_{SN} - \frac{1}{m(\sigma)} \int_{\sigma} \bar{u}_y(s, t_n) ds \right) \right|.$$

In order to estimate the term B_{5A} we use technique from [5]. Let us note that due to simplification we omit the time variable here and provide only necessary arguments, the complete proof can be found in chapter 9.6 of [5]. Let us define $R_{W,\sigma}$ as follows

$$R_{W,\sigma} = \frac{u(x_E) - u(x_W)}{h} - \frac{1}{m(\sigma)} \int_{\sigma} \nabla u(x) \cdot \mathbf{n}_{W,\sigma} ds.$$

Using Taylor expansion and $u \in C^2(\chi_{\sigma})$, cf. Fig. 3.1, we have

$$u(x_E) - u(x) = \nabla u(x) \cdot (x_E - x) + \int_0^1 H(u)[gx + (1-g)x_E](x_E - x) \cdot (x_E - x)g dg$$

and

$$u(x_W) - u(x) = \nabla u(x) \cdot (x_W - x) + \int_0^1 H(u)[gx + (1-g)x_W](x_W - x) \cdot (x_W - x)g dg,$$

where $x \in \sigma$ and $H(u)[z]$ is the Hessian matrix of u at a point z . Subtracting one equation from the other and integrating over σ we get

$$|R_{W,\sigma}| \leq B_{W,\sigma} + B_{E,\sigma},$$

where

$$B_{W,\sigma} = \frac{C}{hm(\sigma)} \int_{\sigma} \int_0^1 |H(u)(gx + (1-g)x_W)| |x_W - x|^2 g dg ds$$

and $B_{E,\sigma}$ is given just changing W to E . To conclude, we note that $x_E - x_W = h\mathbf{n}_{W,\sigma}$. Thanks to the Cauchy-Schwarz inequality and the fact that $|x_W - x| \leq m(\sigma)$ we can bound $B_{W,\sigma}$ in the following way

$$(5.30) \quad |B_{W,\sigma}| \leq \frac{Cm(\sigma)^2}{h^{\frac{3}{2}}} \left(\int_{\chi_{\sigma}} |H(u)[z]|^2 dz \right)^{\frac{1}{2}}.$$

The above mention facts lead to

$$\begin{aligned} |B_{5A}| &\leq \bar{\lambda} \frac{C}{h^2} \int_{\sigma} \int_0^1 |H(u)(gx + (1-g)x_E)(x_E - x) \cdot (x_E - x)g| dg ds \\ &\quad + \bar{\lambda} \frac{C}{h^2} \int_{\sigma} \int_0^1 |H(u)(gx + (1-g)x_W)(x_W - x) \cdot (x_W - x)g| dg ds \\ &\quad + \bar{\beta} \frac{C}{h^2} \sum_{\delta \in P_{\sigma} \cap \mathcal{E}_{int}} \frac{1}{4} \int_{\sigma} \int_0^1 |H(u)(gx + (1-g)x_{E_{\delta}})(x_{E_{\delta}} - x) \cdot (x_{E_{\delta}} - x)g| dg ds \\ &\quad + \bar{\beta} \frac{C}{h^2} \sum_{\delta \in P_{\sigma} \cap \mathcal{E}_{int}} \frac{1}{4} \int_{\sigma} \int_0^1 |H(u)(gx + (1-g)x_{W_{\delta}})(x_{W_{\delta}} - x) \cdot (x_{W_{\delta}} - x)g| dg ds. \end{aligned}$$

Owing to boundedness of the diffusion tensor elements, relation (5.30) and Young's inequality we can estimate the fifth term by

$$|B_5| \leq Ch^{\frac{3}{2}} \sum_{n=1}^m \int_{t_{n-1}}^{t_n} \sum_{\sigma \in \mathcal{E}_{int}} \left(\int_{\chi_\sigma} |H(u)[z]|^2 dz \right)^{\frac{1}{2}} |e_E^n - e_W^n| dt \leq \\ \omega \sum_{n=1}^m \int_{t_{n-1}}^{t_n} \sum_{\sigma \in \mathcal{E}_{int}} \bar{\lambda}_\sigma (e_E^n - e_W^n)^2 dt + C(\omega) h^3 \sum_{n=1}^m \int_{t_{n-1}}^{t_n} \sum_{\sigma \in \mathcal{E}_{int} \chi_\sigma} \int \frac{|H(u)[z]|^2}{\bar{\lambda}_\sigma} dz dt,$$

which gives us

$$(5.31) \quad |B_5| \leq \omega \sum_{n=1}^m \int_{t_{n-1}}^{t_n} \sum_{\sigma \in \mathcal{E}_{int}} \bar{\lambda}_\sigma (e_E^n - e_W^n)^2 + C(\omega) h^3 \|u\|_{L_2(I, H^2(\Omega))}^2 dt.$$

Concerning the last term, we can write

$$B_6 = -2 \sum_{n=1}^m \int_{t_{n-1}}^{t_n} \sum_{\sigma \in \mathcal{E}_{int}} \int_{\sigma} (D\nabla u(s, t_n) - D\nabla u(s, t)) \cdot \mathbf{n}_{W, \sigma} e_W^n ds dt \\ = \sum_{n=1}^m \int_{t_{n-1}}^{t_n} \sum_{\sigma \in \mathcal{E}_{int}} \int_{\sigma} (D\nabla u(s, t_n) - D\nabla u(s, t)) \cdot \mathbf{n}_{W, \sigma} (e_E^n - e_W^n) ds dt,$$

which can be split in the form

$$B_6 \leq C(\omega) \sum_{n=1}^m \int_{t_{n-1}}^{t_n} \sum_{\sigma \in \mathcal{E}_{int}} \int_{\sigma} ((D\nabla u(s, t_n) - D\nabla u(s, t)) \cdot \mathbf{n}_{W, \sigma})^2 \frac{m(\sigma)}{\bar{\lambda}_\sigma} ds dt \\ + \frac{\omega}{2} \sum_{n=1}^m \int_{t_{n-1}}^{t_n} \sum_{\sigma \in \mathcal{E}_{int}} \bar{\lambda}_\sigma (e_E^n - e_W^n)^2 dt$$

by the Young inequality. Properties of the matrix D together with the regularity of the solution u lead to the following estimate for the first term

$$C(\omega) \sum_{n=1}^m \int_{t_{n-1}}^{t_n} \sum_{\sigma \in \mathcal{E}_{int}} \int_{\sigma} ((D\nabla u(s, t_n) - D\nabla u(s, t)) \cdot \mathbf{n}_{W, \sigma})^2 \frac{m(\sigma)}{\bar{\lambda}_\sigma} ds dt \\ \leq C(\omega) \sum_{n=1}^m \int_{t_{n-1}}^{t_n} \sum_{\sigma \in \mathcal{E}_{int}} \int_{\sigma} \left(\int_t^{t_n} \frac{\partial \nabla u(s, g)}{\partial g} dg \right)^2 m(\sigma) ds dt \\ \leq C(\omega) k \sum_{n=1}^m \int_{t_{n-1}}^{t_n} \sum_{\sigma \in \mathcal{E}_{int}} \int_{\sigma} \int_{t_{n-1}}^{t_n} \left(\frac{\partial \nabla u(s, g)}{\partial g} \right)^2 dg m(\sigma) ds dt \\ \leq C(\omega) k^2 \|\nabla u_t\|_{L_2(I, L_\infty(\Omega))},$$

where lower limit of the integration $t \in (t_{n-1}, t_n]$. And from the above mentioned inequalities we get

$$(5.32) \quad B_6 \leq C(\omega)k^2\|\nabla u_t\|_{L_2(I, L_\infty(\Omega))} + \frac{\omega}{2} \sum_{n=1}^m \int_{t_{n-1}}^{t_n} \sum_{\sigma \in \mathcal{E}_{int}} \bar{\lambda}_\sigma (e_E^n - e_W^n)^2 dt.$$

At the end, we apply (5.9), (5.10), (5.28), (5.29), (5.31) and (5.32) in (5.8) to state that for ω sufficiently small (e.g. for $\omega \leq \frac{1}{20}$)

$$\begin{aligned} & \int_{\Omega} |e_{h,k}^m|^2 dx + \sum_{n=1}^m \int_{\Omega} |e_{h,k}^n - e_{h,k}^{n-1}|^2 dx + \sum_{n=1}^m \int_{t_{n-1}}^{t_n} \sum_{\sigma \in \mathcal{E}_{int}} \bar{\lambda}_\sigma (e_E^n - e_W^n)^2 dt \\ & \leq C \int_{\Omega} |e_{h,k}^0|^2 dx + C(k + h^2) + C \sum_{n=1}^m \int_{t_{n-1}}^{t_n} \int_{\Omega} |e_{h,k}^n|^2 dx dt. \end{aligned}$$

Since for the initial error we have

$$\int_{\Omega} |e_{h,k}^0|^2 dx \leq Ch^2$$

thanks to Gronwall's lemma we end up the proof. \square

6. Numerical experiments. In this section, we are going to demonstrate practical advantages of our numerical scheme. To that goal we present and discuss the results of several computational experiments performed by the scheme. The results show that the diffusion improves the structure connectivity which enables to get good segmentation of biological images.

The images used for these experiments come from the two-photon laser scanning microscopy. They represent the corresponding cell membranes, cf. Fig. 6.1 (top left), nuclei, cf. Fig. 6.1 (middle, left). In order to provide a segmentation we can also put membranes and nuclei together and form one coupled image, cf. Fig. 6.1 (bottom left). These 2D slices were chosen from 3D images showing early stages of the zebrafish embryogenesis.

In experiments with our scheme for the nonlinear tensor anisotropic diffusion we use the spatial step $h = 0.01$, time step $k = 0.0001$, $C = 1$, $\alpha = 0.001$, $\tilde{t} = 10^{-5}$, $\rho = 0.002$ for the membranes and coupled images and $\tilde{t} = 10^{-10}$, $\rho = 0.1$ for the nuclei images. The arising linear systems are solved by the Gauss-Seidel iterations.

Figs. 6.1 and 6.2 demonstrate the behaviour of the nonlinear tensor anisotropic diffusion applied to these 2D images. We can observe that this type of multiscale process enhances the connectivity of the zebrafish embryo eye retina structures boundaries while smoothing their interior. It enables to get much better results of the image segmentation algorithms which depend on the structure connectivity. The most expressive example of this connectivity improvement is represented by the processed nuclei image and therefore we display the nuclei images in the enlarged form, cf. Fig. 6.2. Although, in Fig. 6.2 (top), we can see only separate nuclei, we are able to recognize the embryo structures in the original image. However, this simple task for a human brain is nontrivial for the image segmentation algorithms. As we can see, it can be overcome by pre-processing using the nonlinear tensor diffusion, cf. Fig. 6.2 (bottom).

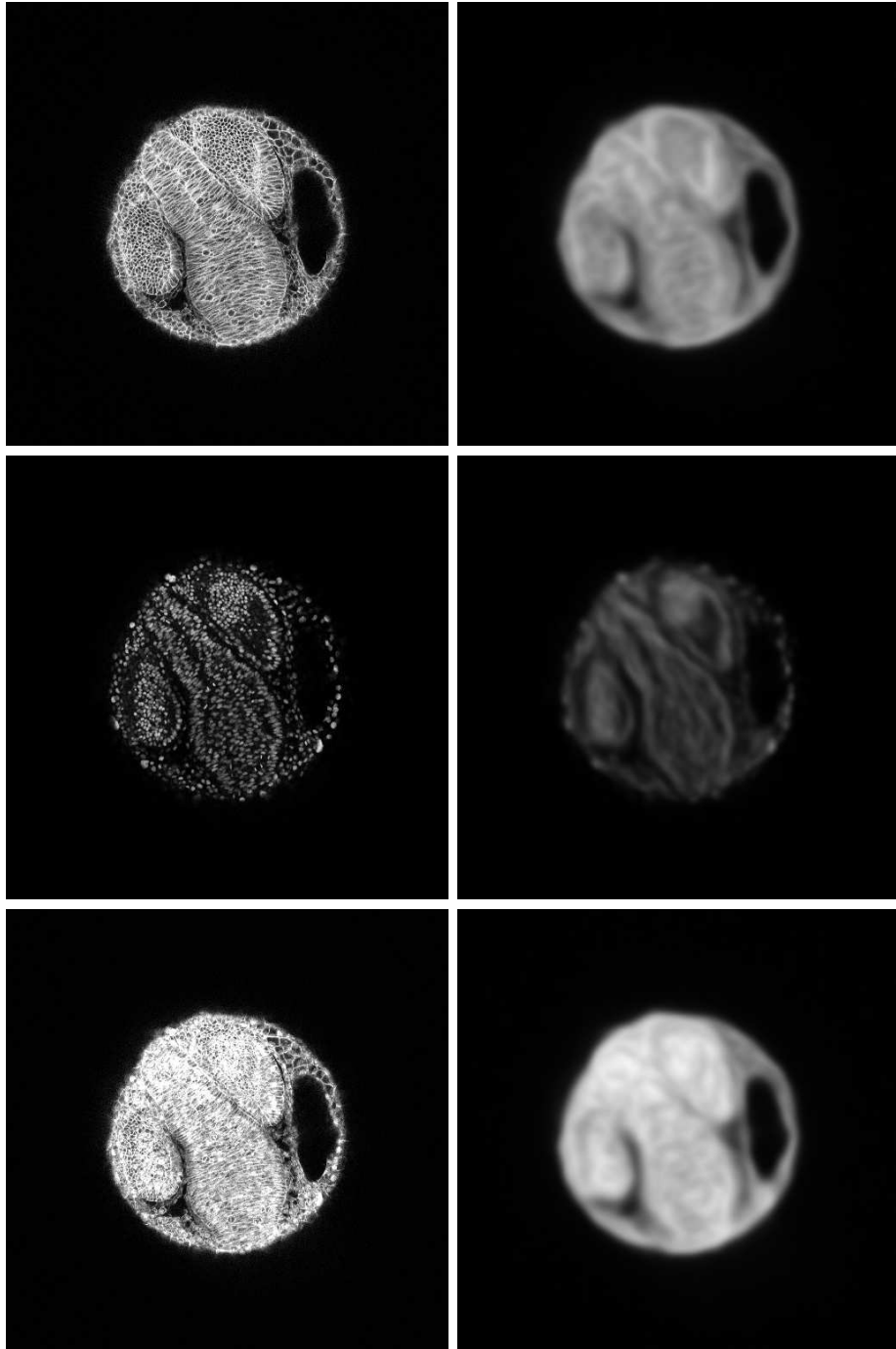


FIG. 6.1. *2D slices of the 3D zebrafish embryo image. Left: original images. Right: filtered images after 50 time steps. Top: cell membranes. Middle: cell nuclei. Bottom: membranes and nuclei coupled together.*

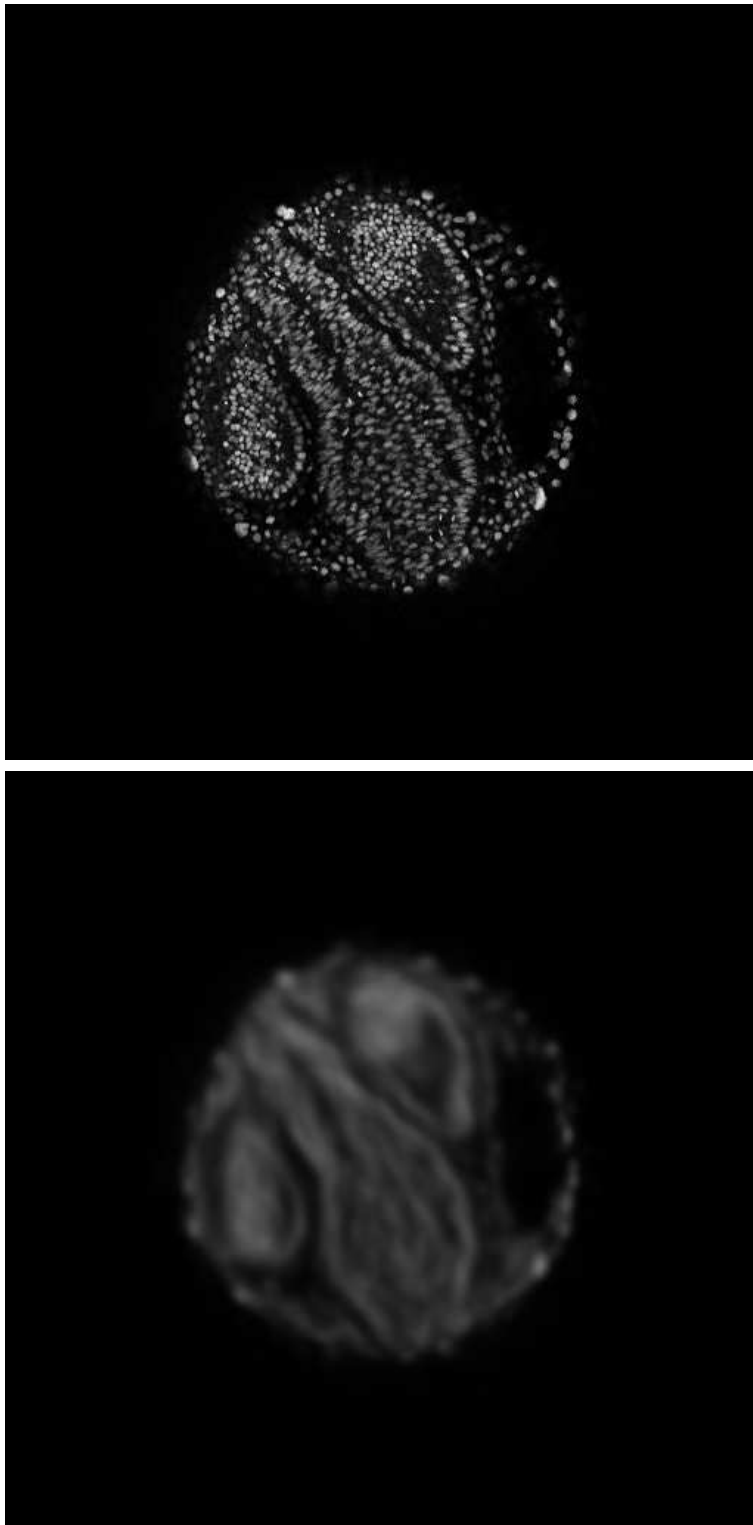


FIG. 6.2. *The images of cell nuclei from the Fig. 6.1.*

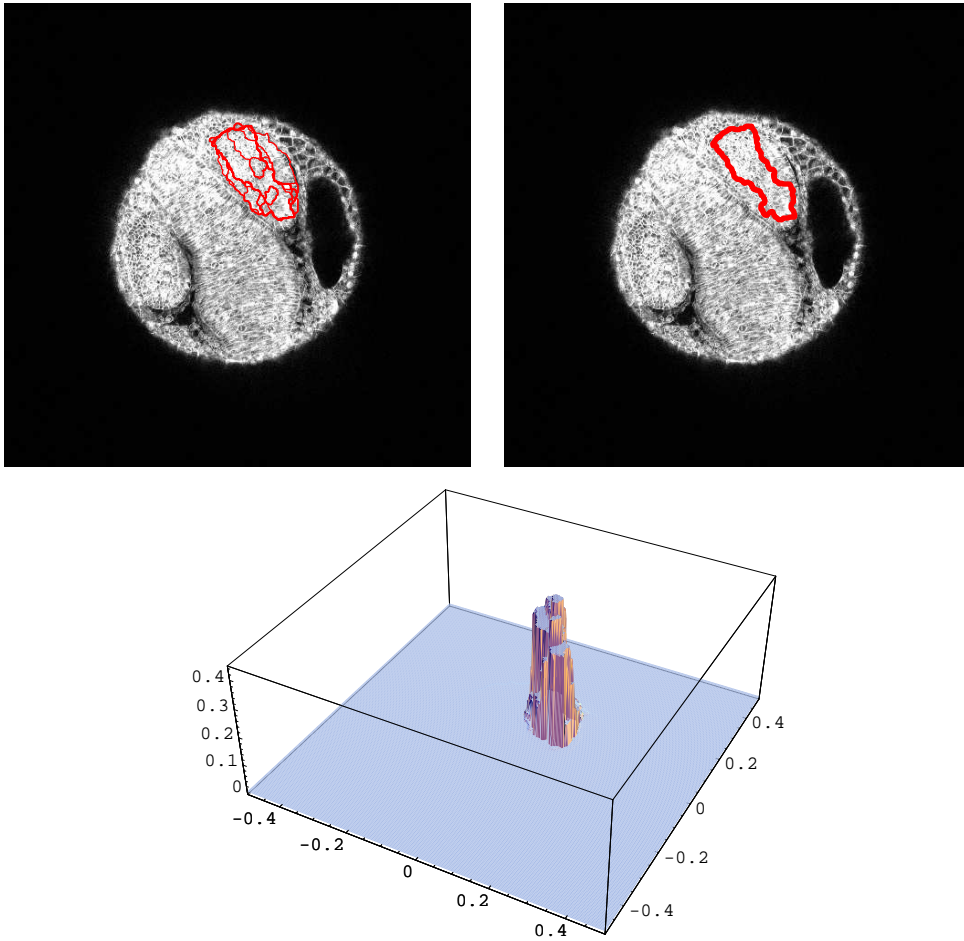


FIG. 6.3. *The structure segmentation for the original image of coupled membranes and nuclei. Top (left): the isolines of the final state of segmentation function. Top (right): the chosen isoline of the final state of segmentation function. Bottom: the graph of the final state of segmentation function. The results were obtained after 5000 segmentation steps.*

In Figs. 6.3-6.6 we present the image segmentation results in order to show how one can exploit improvement of the connectivity of coherent structures. We use the image segmentation algorithm based on the subjective surface method [18] and its semi-implicit finite volume implementation [14]. We start the segmentation constructing an initial segmentation function centered in a segmented object. Then, in order to extract a shape of the object, we evolve it by solving the so-called subjective surface equation which is a special geometrical partial differential equation for moving graphs by weighted mean curvature, cf. [18, 14]. Its solution evolves to a final state with a shock profile which gives the segmentation result. To extract the shape of the segmented object we take a proper isoline of the shock profile at the stopping time, mostly naturally the average of maximal and minimal value of the final segmentation function.

In Fig. 6.3 we present the segmentation results obtained using the original image of coupled membranes and nuclei, cf. Fig. 6.1 (bottom left). Due to a great number

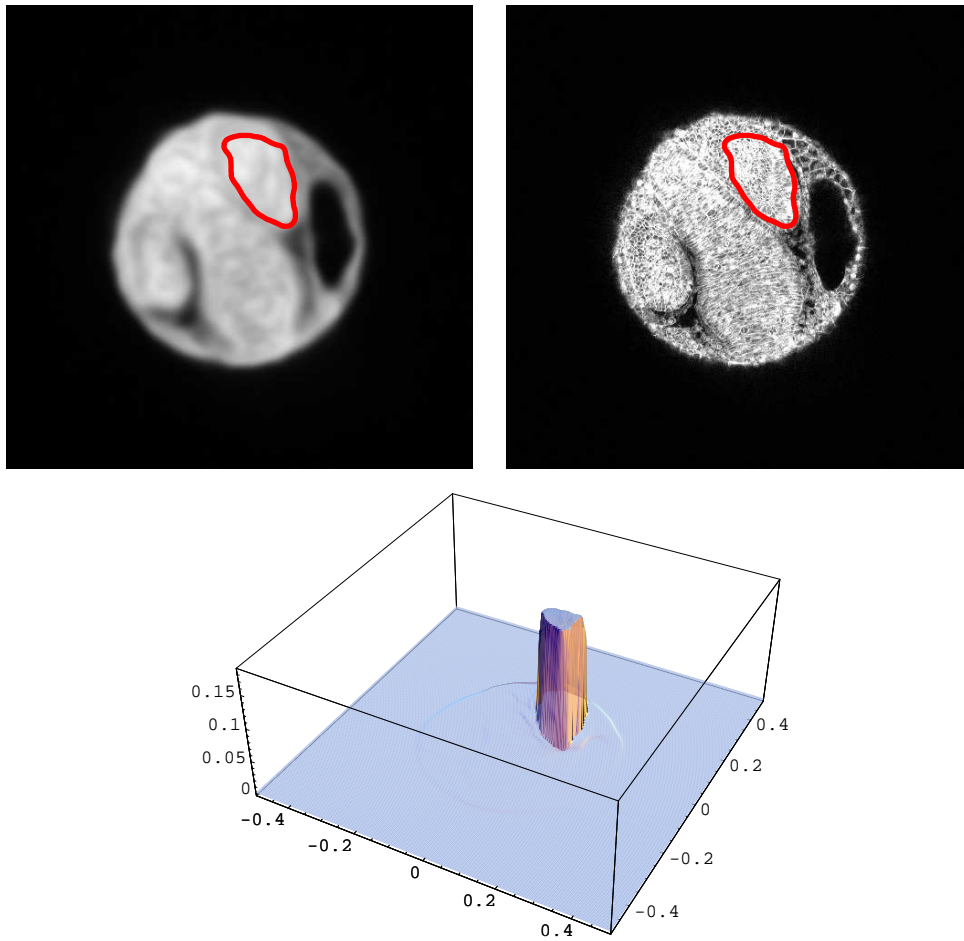


FIG. 6.4. *The structure segmentation for the filtered image of coupled membranes and nuclei. Top (left): the chosen isoline of the final state of segmentation function. Top (right): the same isoline of the final state of segmentation function displayed on the original image. Bottom: the graph of the final state of segmentation function. The results were obtained after 200 segmentation steps.*

of noisy structures as well as structures represented by individual membranes and nuclei in the original image, the segmentation algorithm is not able to find the correct boundary of the segmented embryo structure. The isolines of the final state of segmentation function are depicted at the top left of the figure, the mean isoline at the top right and the graph of the final state of segmentation function at the bottom of the figure.

We can compare this segmentation result with the ones obtained using the filtered images presented in Figs. 6.4-6.6. The mean isoline of the final state of segmentation function is shown at the top of the figures, where we display it together with the filtered image (top left) and with the original one (top right). The graph of the final state of segmentation function is shown at the bottom of the figures. As one can clearly see, almost all isolines are accumulated along the structure boundary due to the correct shock profile obtained using the filtered image and thus the mean isoline

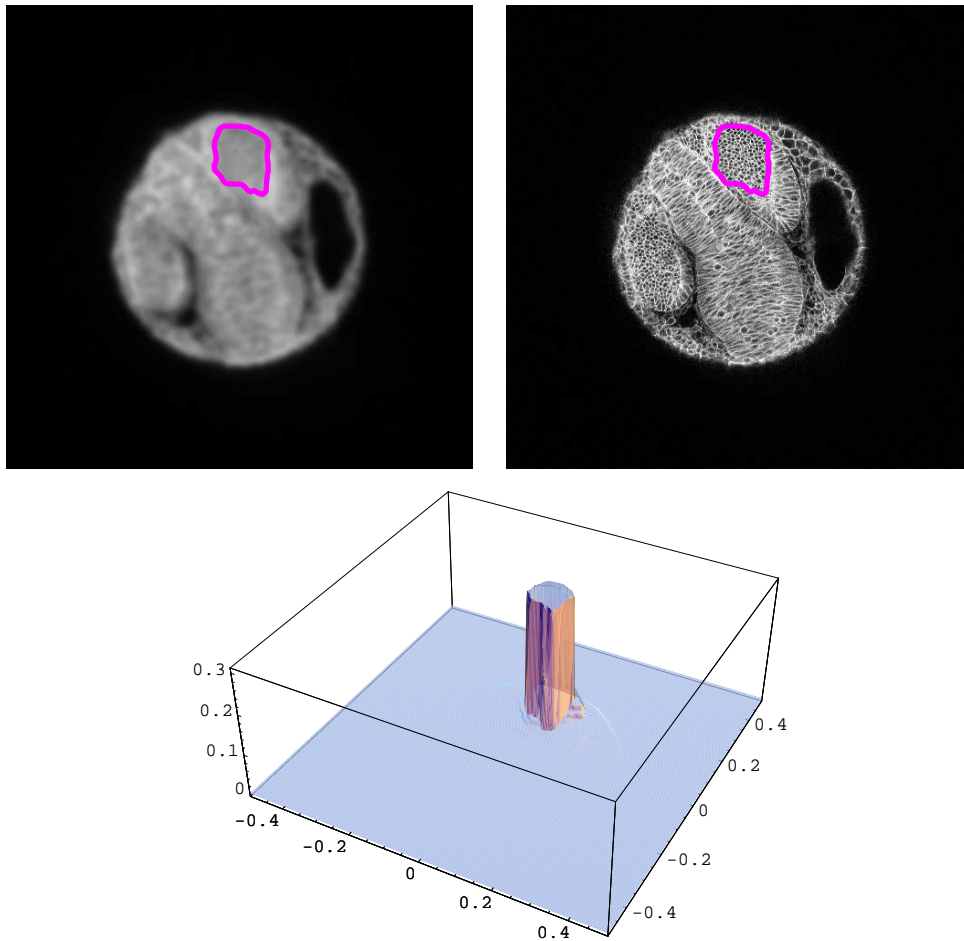


FIG. 6.5. The structure segmentation for the filtered image of membranes. Top (left): the chosen isoline of the final state of segmentation function. Top (right): the same isoline of the final state of segmentation function displayed on the original image. Bottom: the graph of the final state of segmentation function. The results were obtained after 200 segmentation steps.

correctly represents the biological structure.

7. Acknowledgement. This paper was supported by the European projects Embryomics and BioEmergences, the grants APVV-RPEU-0004-06, APVV-0351-07, APVV-LPP-0020-07 and the grant of VEGA 1/3321/06. We thank Dr. Nadine Peyrieras from CNRS Paris for providing the testing images.

REFERENCES

- [1] L. ALVAREZ, F. GUICHARD, P. L. LIONS AND J. M. MOREL, *Axioms and Fundamental Equations of Image Processing*, Arch. Rat. Mech. Anal., Vol. 123 (1993) pp. 200-257.
- [2] F. CATTÉ, P. L. LIONS, J. M. MOREL AND T. COLL, *Image selective smoothing and edge detection by nonlinear diffusion*, SIAM J. Numer. Anal. 29 (1992), pp. 182-193.
- [3] Y. COUDIERE, J. P. VILA AND P. VILLEDIEU, *Convergence rate of a finite volume scheme for a two-dimensional convection-diffusion problem*, M2AN Math. Model. Numer. Anal., 33, (1999) pp. 493-516.

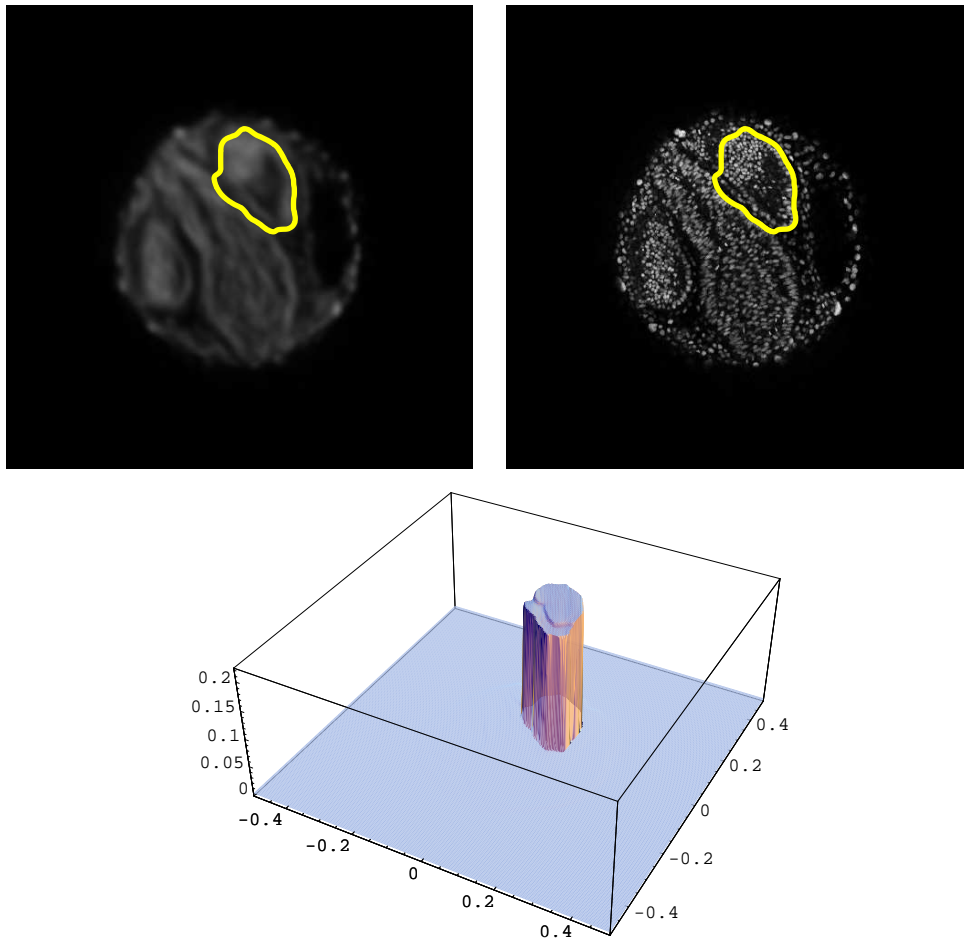


FIG. 6.6. The structure segmentation for the filtered image of nuclei. Top (left): the chosen isoline of the final state of segmentation function. Top (right): the same isoline of the final state of segmentation function displayed on the original image. Bottom: the graph of the final state of segmentation function. The results were obtained after 2500 segmentation steps.

- [4] O. DRBLÍKOVÁ AND K. MIKULA, *Convergence Analysis of Finite Volume Scheme for Nonlinear Tensor Anisotropic Diffusion in Image Processing*, SIAM Journal on Numerical Analysis, Vol. 46, No. 1, (2007) pp. 37–60.
- [5] R. EYMARD, T. GALLOUËT AND R. HERBIN, *Finite Volume Methods*, in: Handbook for Numerical Analysis, Vol. 7 (Ph. Ciarlet, J. L. Lions, eds.), Elsevier, (2000).
- [6] G. GILBOA, N. SOCHEN AND Y. Y. ZEEVI, *Forward-and-backward diffusion processes for adaptive image enhancement and denoising*, IEEE Trans. Image Processing 11 (7), (2002) pp. 689–703.
- [7] A. HANDLOVIČOVÁ AND Z. KRIVÁ, *Error estimates of finite volume scheme for Perona-Malik equation*, Acta Math. Univ. Comenianae, Vol. 74, No. 1, (2005) pp. 79–94.
- [8] J. KAČUR AND K. MIKULA, *Solution of nonlinear diffusion appearing in image smoothing and edge detection*, Applied Numerical Mathematics 17, (1995) pp. 47–59.
- [9] Z. KRIVÁ, *Explicit finite volume scheme for the Perona-Malik equation*, Computational Methods in Applied Mathematics, Vol. 5, No. 2, (2005) pp. 170–200.
- [10] Z. KRIVÁ AND K. MIKULA, *An adaptive finite volume scheme for solving nonlinear diffusion equations in image processing*, Journal for Visual Communication and Image Representation, Vol. 13, No.1/2 (2002) pp.22–35.

- [11] O. A. LADYŽENSKAJA, V. SOLONNIKOV AND N. N. URAĽCEVA, *Linear and quasilinear equations of parabolic type*, Nauka, Moskva, (1967), (in Russian).
- [12] C. LANGE AND K. POLTHIER, *Anisotropic smoothing of point sets. Com. Geom. Design* 22 (7), (2005) pp. 680–692.
- [13] K. MIKULA AND N. RAMAROSY, *Semi-implicit finite volume scheme for solving nonlinear diffusion equations in image processing*, Numer. Math. 89 (3), (2001) pp. 561–590.
- [14] K. MIKULA, A. SARTI, F. SGALLARI, *Co-volume level set method in subjective surface based medical image segmentation*, in: Handbook of Medical Image Analysis: Segmentation and Registration Models (J. Suri et al., Eds.), Springer, New York, (2005) pp. 583–626.
- [15] P. PERONA AND J. MALIK, *Scale space and edge detection using anisotropic diffusion*, in Proc. IEEE Computer Society Workshop on Computer Vision (1987).
- [16] T. PREUSSER AND M. RUMPF, *An adaptive finite element method for large scale image processing*, Journal of Visual Comm. and Image Repres., 11, (2000) pp. 183–195.
- [17] T. PREUSSER AND M. RUMPF, *A level set method for anisotropic geometric diffusion in 3D image processing*, SIAM J. Appl. Math 62 (5), (2002) pp. 1772–1793.
- [18] A. SARTI, R. MALLADI, J. A. SETHIAN, *Subjective Surfaces: A Method for Completing Missing Boundaries*, Proceedings of the National Academy of Sciences of the United States of America, Vol. 12, No. 97 (2000) pp. 6258–6263.
- [19] J. WEICKERT, *Anisotropic Diffusion in Computer Vision*, Teubner-Stuttgart, (1998).
- [20] J. WEICKERT, *Coherence-enhancing diffusion filtering*, Int. J. Comput. Vision, Vol. 31, (1999) pp. 111–127.